Lophiostroma schmidtii (NICHOLSON)
THE MOST ENIGMATIC PALAEOZOIC STROMATOPOROID: TAXONOMY, GROWTH & DIAGENESIS
& comparisons with some of its friends

PART 2 of 2

Stephen Kershaw
Brunel University London; and Natural History Museum, London, UK

Reconstruction of structure and diagenesis of *Lophiostroma schmidtii* [this picture is repeated later with caption]

They say you shouldn't judge a book by its cover, and in this case by its title; this apparently highly specialised account contains a lot of basic knowledge and questions about stromatoporoids

An atlas of images from the Hemse group, Ludlow, Silurian, in the Kuppen peninsula biostromes, eastern Gotland, Sweden; and some other Silurian samples from Gotland and UK

This document is a compendium of annotated images and interpretations intended as a palaeontological and sedimentological research tool

Version 01; MONTH 2022; **CC-BY-4.0 licence**

6.9. Case Study 9: K4b

This case shows further examples of diagenesis of *Ls*, using different orientations of XPL views, contacts with encrusting *Ps* and primary cavity cements.

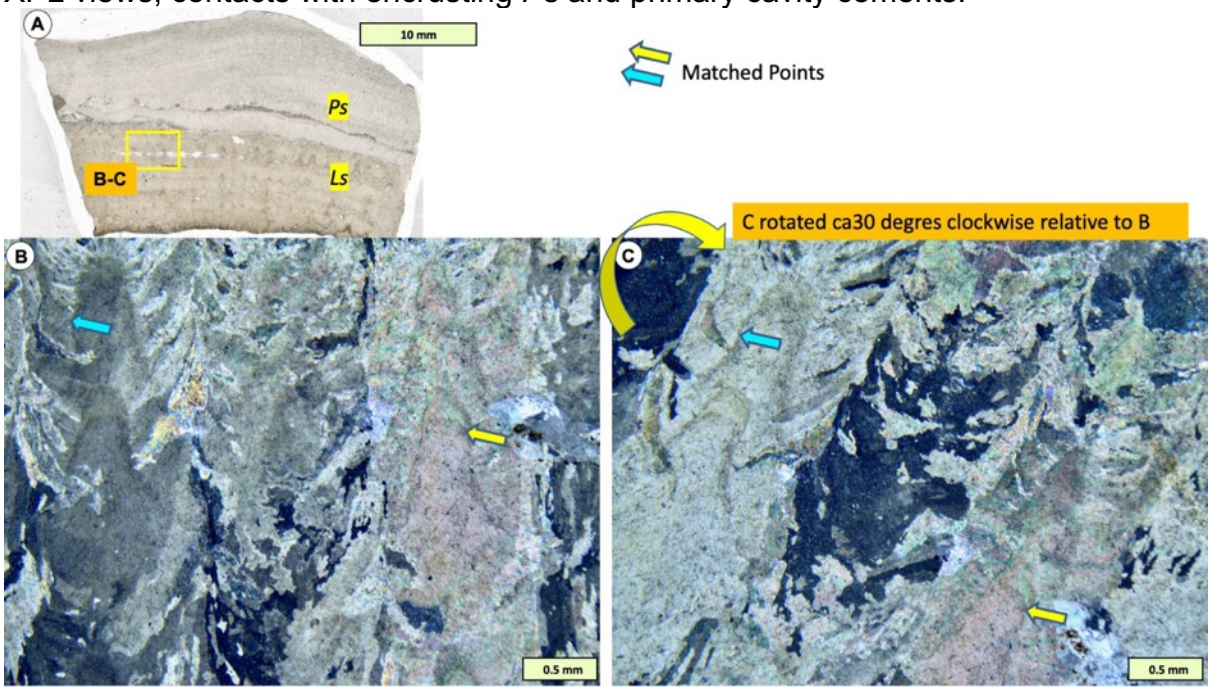

Fig. 6.9-1A-C. VS views of *Ls* in XPL showing large crystals of diagenetic alteration passing through the growth layers (blue & yellow arrows are matched points). File: 16-1-Case09-K4b-i-ii-Ls-VS

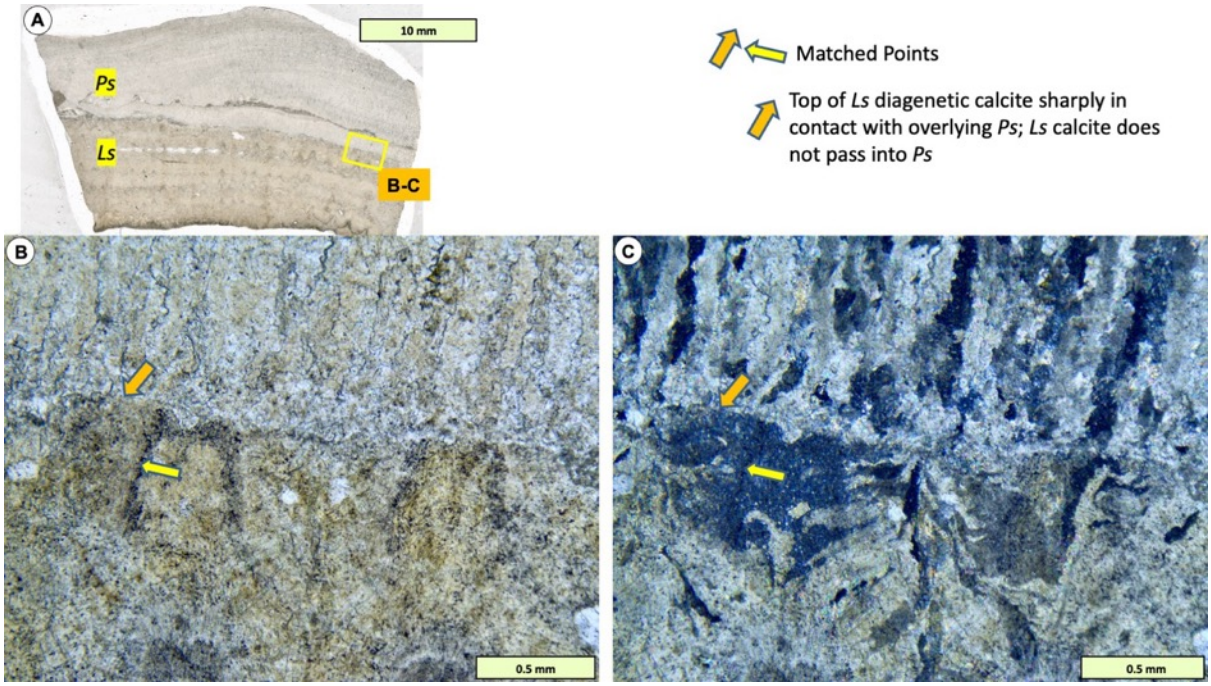

Fig. 6.9-2A-C. Contact between upper surface of *Ls* and encrusting *Ps* (orange & yellow arrows are matched points). The papillae of *Ls* are apparently truncated, but 1) other images show papillae did not form in all cases on *Ls* surfaces; and 2) the slightly irregular nature of the contact looks like this is

a stylolitised contact; so in this part of the sample pressure solution may have influenced the final result. Note contrast between diagenetic style of *Ls* and *Ps*. File: 16-2-Case09-K4b-i-ii-Ls-VS

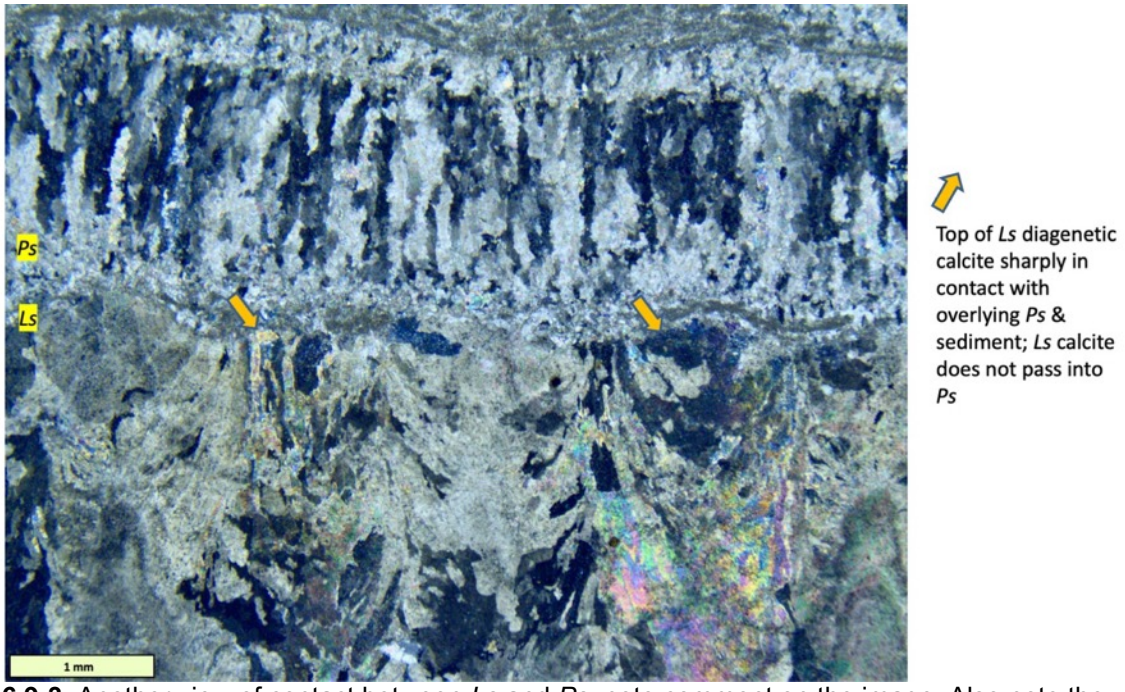

Fig. 6.9-3. Another view of contact between *Ls* and *Ps*, note comment on the image. Also note the diagenetic alteration in the *Ps* does not pass through the growth interruption surface. File: 16-3-Case09-K4b-i-ii-Ls-VS

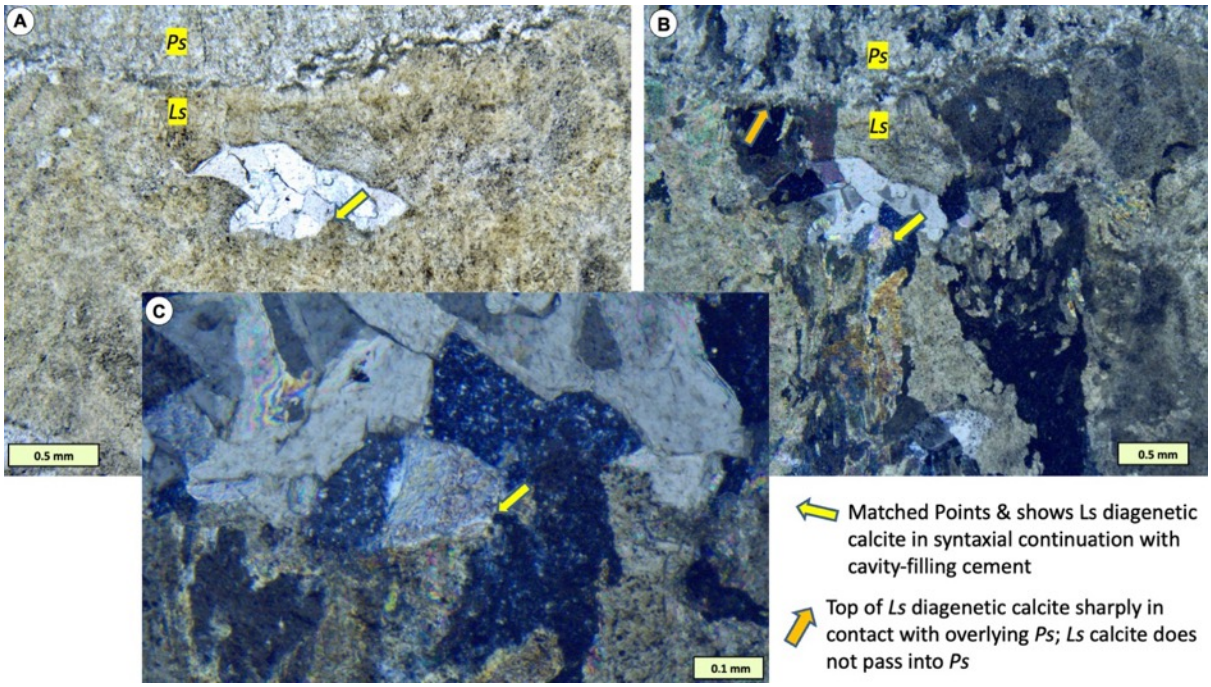

Fig. 6.9-4. Small primary cavity in the Ls has cement infill passing with optical continuity into the Ls skeleton, interpreted to indicate that the cavity was empty until the Ls underwent diagenesis, thus interpreted to be an early process in the rock history. File: 16-4-Case09-K4b-i-ii-Ls-VS

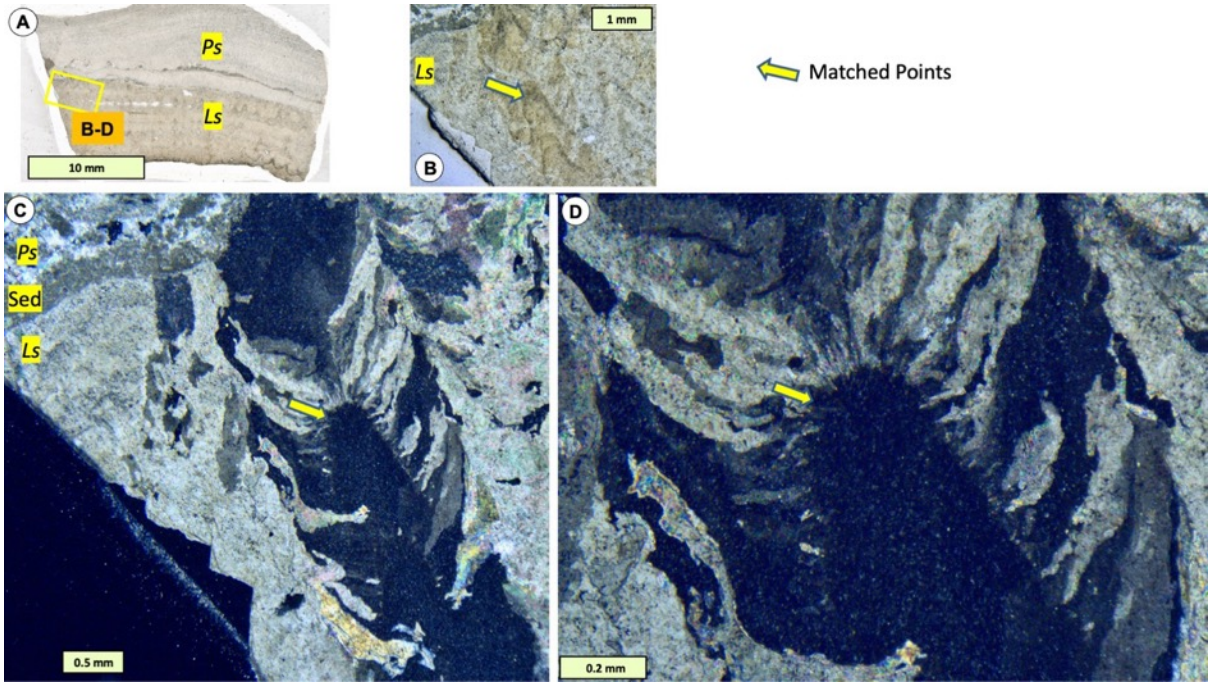

Fig. 6.9-5. Edge of Ls, where the thin section was a little thinner, showing spectacular clarity of the 3D crystal fans in VS, and the interpreted alteration to larger crystals by aggrading neomorphism. However this sample shows an excellent view of the central part being a single crystal but there is some indication that it originally comprised 3D crystal fans, seen in the left photo C. File: 16-5-Case09-K4b-i-ii-Ls-VS

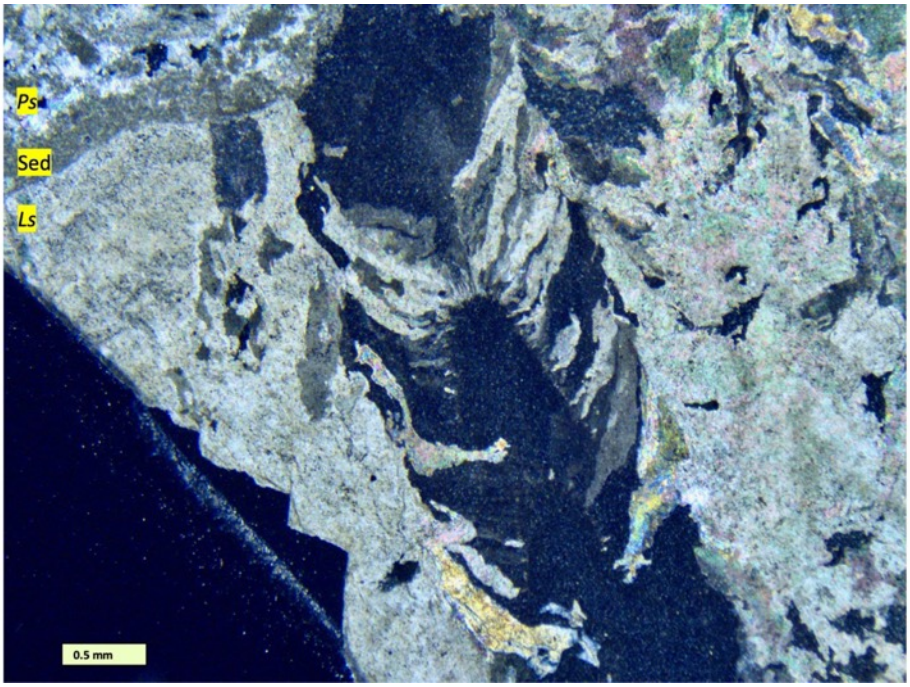

Fig. 6.9-6. Enlargement of Fig. 6.9-5C showing the central part of the column in extinction is **not** a fully singe crystal but has some indication of upward-expanding crystal fans, that are here interpreted as indicating that this crystal was originally a mass of 3D crystal fans. File: 16-6-Case09-K4b-i-ii-Ls-VS

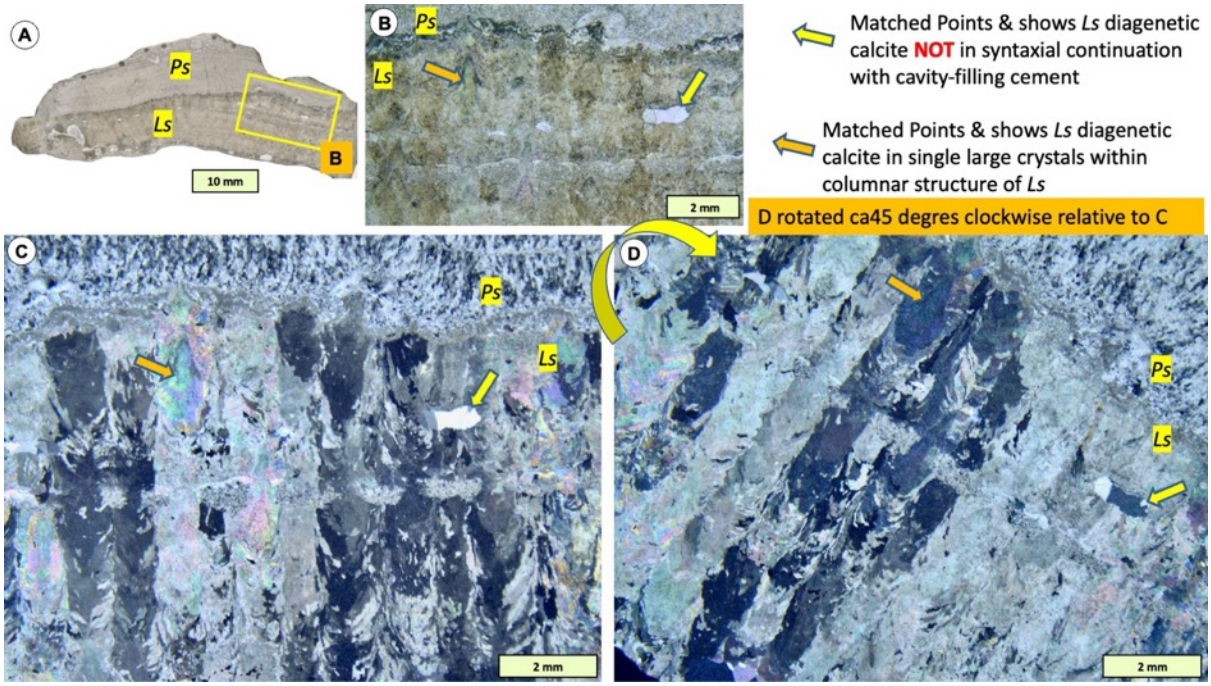

Fig. 6.9-7. VS of *Ls* in XPL in different orientations, showing diagenetic alteration passing through a large thickness of the skeleton, and the interpreted aggrading neomorphic structure of abutting crystals competing for space. File: 16-6-Case09-K4b-i-ii-Ls-VS

6.10. Case Study 10: 3c5-9.45

This case from the lower part of the biostrome at Kuppen 5 shows *Ls* in VS and TS, and demonstrates the standard diagenetic overprinting of 3D crystal fans that are interpreted to have been affected by subsequent aggrading neomorphic structure. Also there is presence of another form of alteration that is overprinted by the 3D crystal fans and subsequent aggrading change; this is loosely called “vaguely-fibrous calcite” in this atlas, pending a more appropriate scientific carbonate term. Thus the evidence in this sample in both VS & TS is of three forms of alteration of the original *Ls* skeletal structure that occur in this sequence: 1) vaguely fibrous calcite; 2) 3D crystal fans; and finally 3) aggrading neomorphic development of large contiguous crystals that abut each other in competitive growth, resulting in the vertical large crystals ubiquitous in *Ls*.

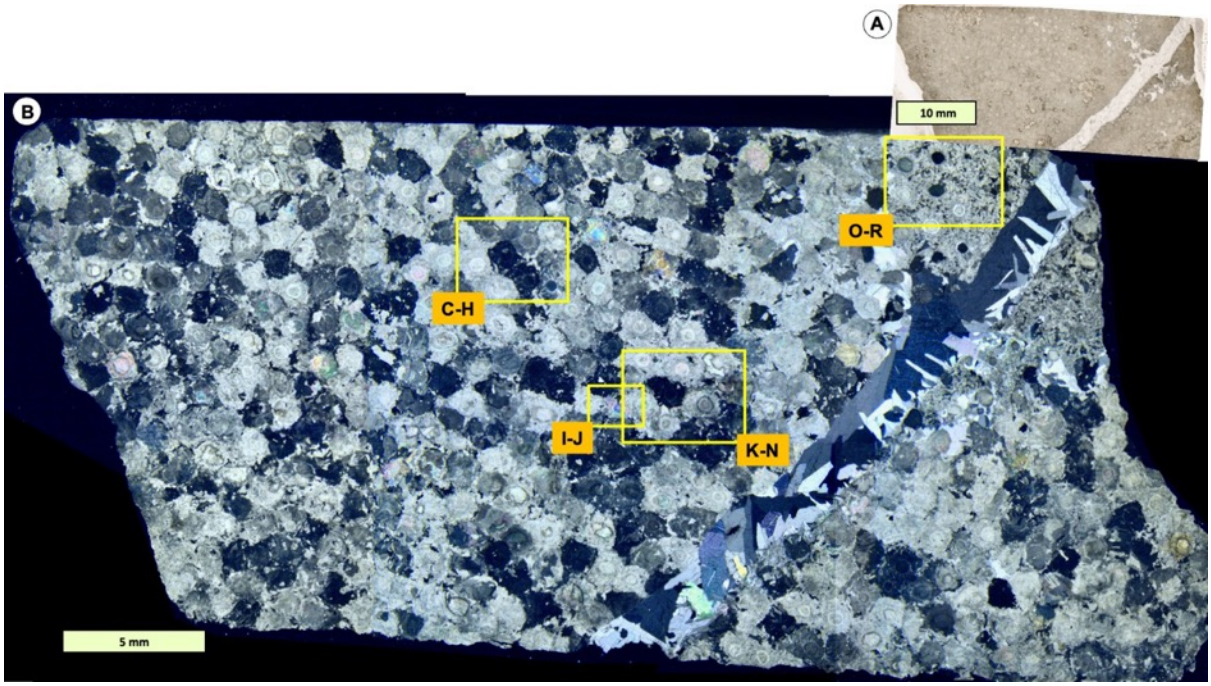

Fig. 6.10-1A-B. TS of whole thin section showing variation of preservation of Ls: 1) Upper right corner (yellow box labelled O-R) shows 3D crystal fans in TS, with large crystal centres that lie in the apex areas of the tight upcurved Ls lamination seen later in the VS views of this specimen. 2) Left margin shows large crystals with a scattering of small crystals included; these are interpreted as the alteration of 3D crystal fans into aggrading neomorphic calcite, that is not completed in this part of the thin section. 3) In upper centre the large crystals do not show the scattering of small crystals, and are interpreted as the final stage of neomorphism. However, in the centre (box labelled K-N) is an area containing the earlier vaguely-fibrous calcite that is not clearly visible in this image because it is overprinted by the aggrading neomorphic texture. On right side is a diagonal fracture filled with calcite that is a mixture of blocky and acicular crystals. It is not clear why there are acicular crystals here. Section 9 of this atlas shows some small gypsum crystals and gypsum pseudomorphs in calcite, potential evidence for raised salinity in the environment of growth of the stromatoporoids in the Hemse Group biostromes. File: 17-01-Case10-3c5-9.45-Ls-VS-TS

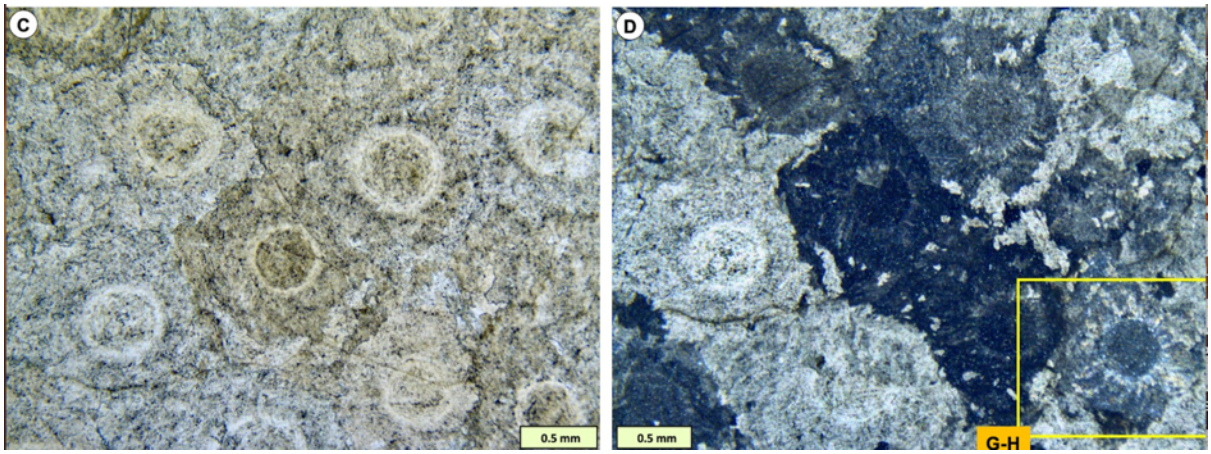

Fig. 6.10-1C-D. TS enlargements of box in Fig. 6.10B, showing PPL and XPL demonstrating contiguous crystals interpreted as aggraded neomorphic structure with a scatter of small crystals (centre) and preservation of radiating crystals (especially seen in yellow box), but also present in most of the other crystals in this view. File: 17-02-Case10-3c5-9.45-Ls-VS-TS-Cut

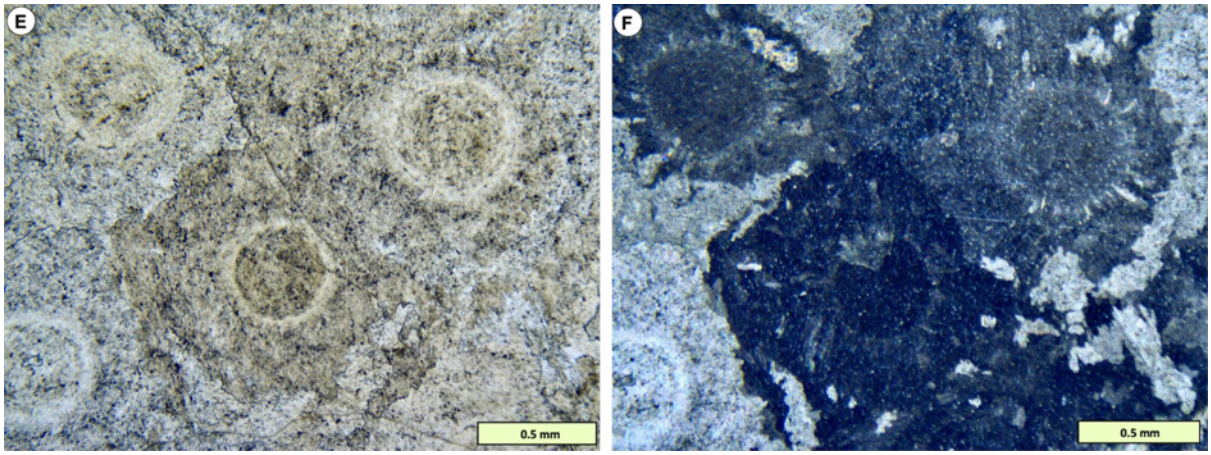

Fig. 6.10-1E-F. Enlargements of C & D showing a bit more detail. File: 17-03-Case10-3c5-9.45-Ls-VS-TS-Cut

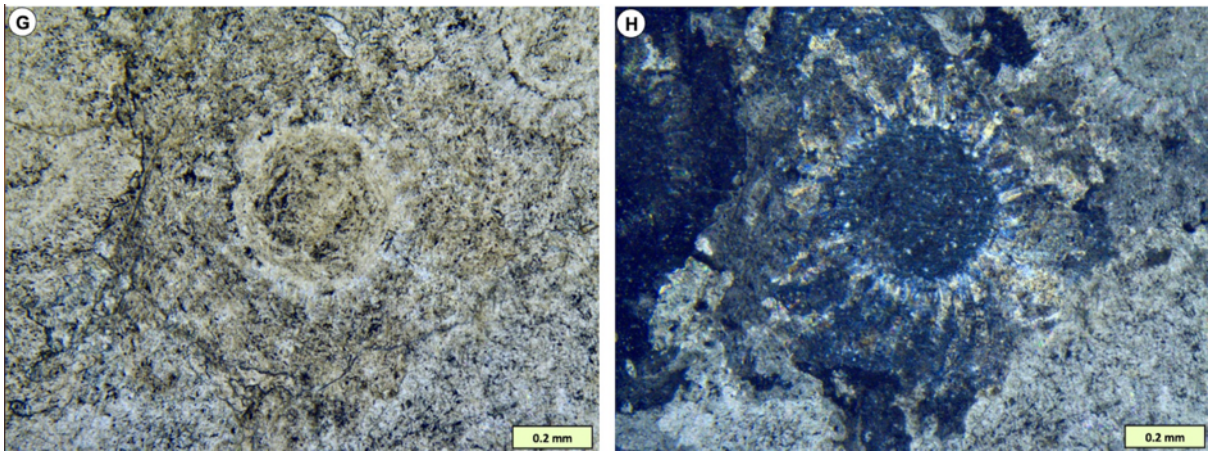

Fig. 6.10-1G-H. Detail of box in D, showing the radial crystals in TS, that are the radiating fans in VS, together indicating 3D crystal fans of the early diagenesis of Ls. 17-04-Case10-3c5-9.45-Ls-VS-TS-Cut

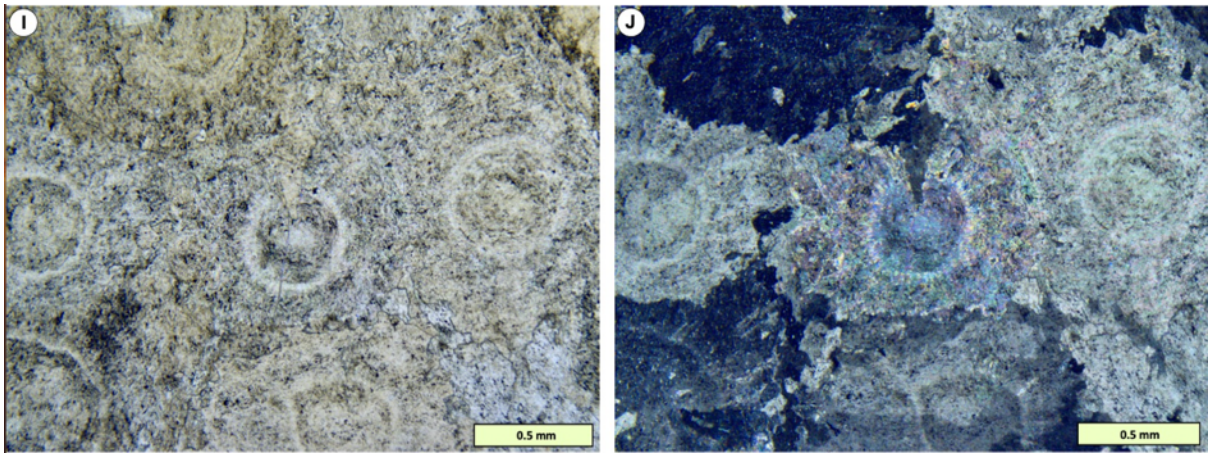

Fig. 6.10-1I-J. TS views showing contiguous comprise boundaries of adjacent crystals of the interpreted aggrading neomorphic alteration of *Ls.* File: 17-05-Case10-3c5-9.45-Ls-VS-TS-Cut

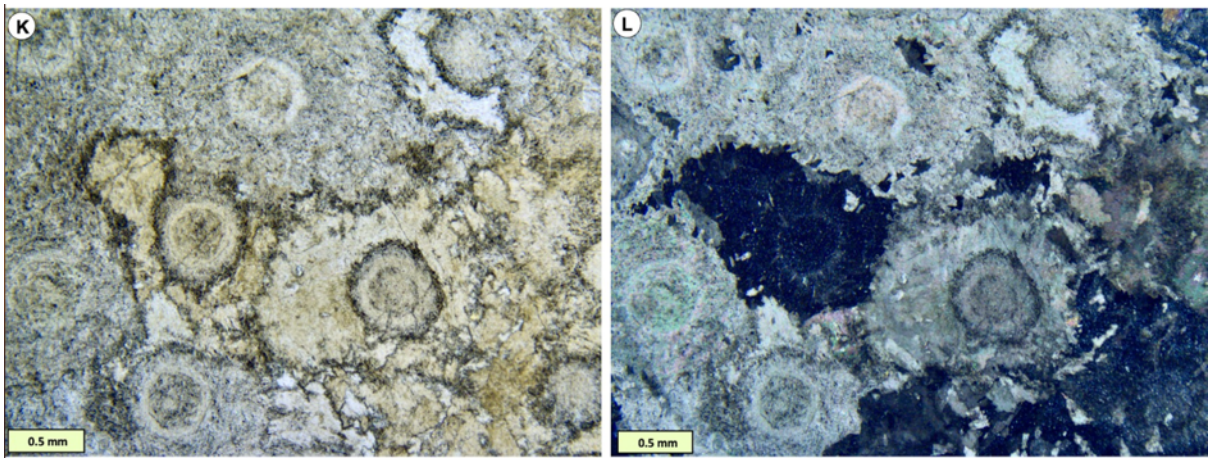

Fig. 6.10-1K-L. Detail of box in Fig. 6-10-1B showing the earliest diagenetic feature called “vaguely-fibrous calcite” (doesn’t look fibrous in this TS view). that is influenced by skeletal texture of Ls papillae centres, but is overprinted by the aggrading neomorphic alteration. File: 17-06-Case10-3c5-9.45-Ls-VS-TS-Cut

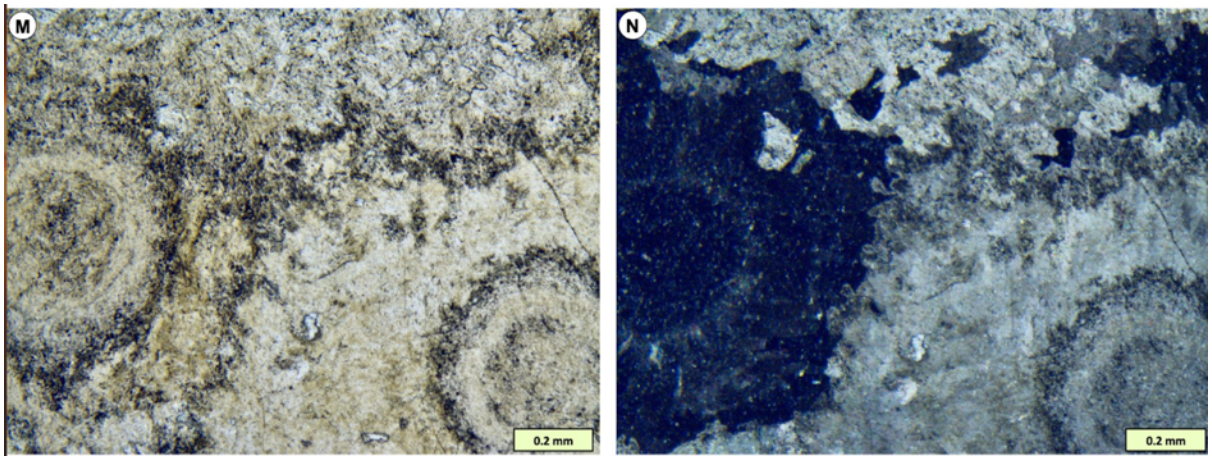

Fig. 6.10-1M-N. Close-up of previous figure showing more detail. Shows the “vaguely-fibrous calcite” is overprinted by FRIC. File:17-07-Case10-3c5-9.45-Ls-VS-TS-Cut

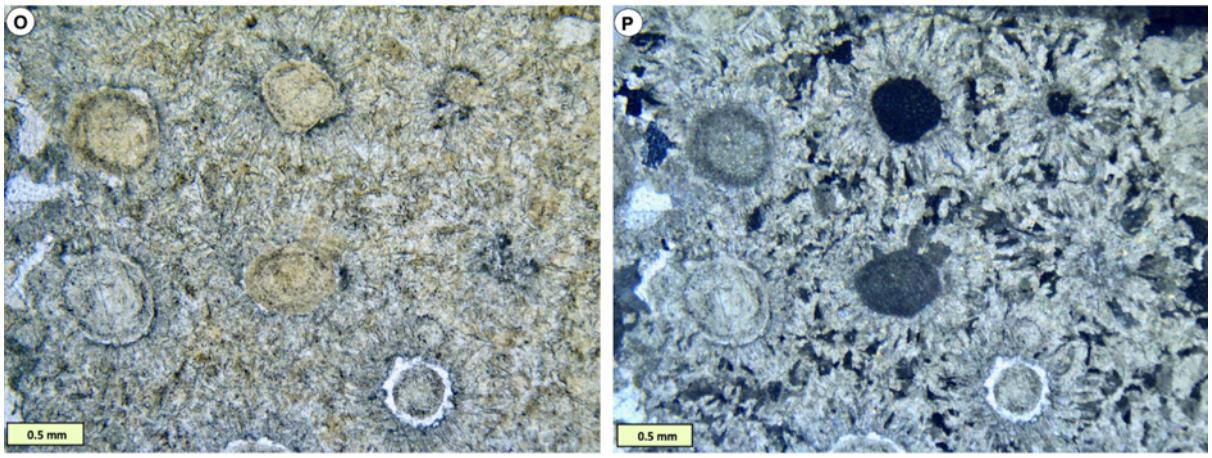

Fig. 6.10-1O-P. Details of radial crystal fans in TS, radiating from single crystal centres. Note the variations. File: 17-08-Case10-3c5-9.45-Ls-VS-TS-Cut

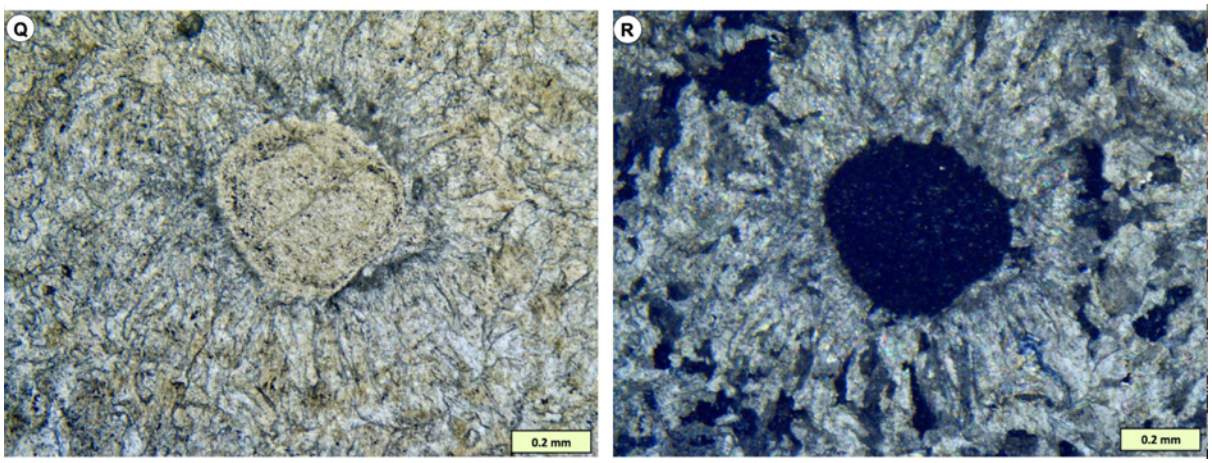

Fig. 6.10-1Q-R. Fine details of previous figure highlighting the radiating crystals visible in both PPL and XPL. File: 17-09-Case10-3c5-9.45-Ls-VS-TS-Cut

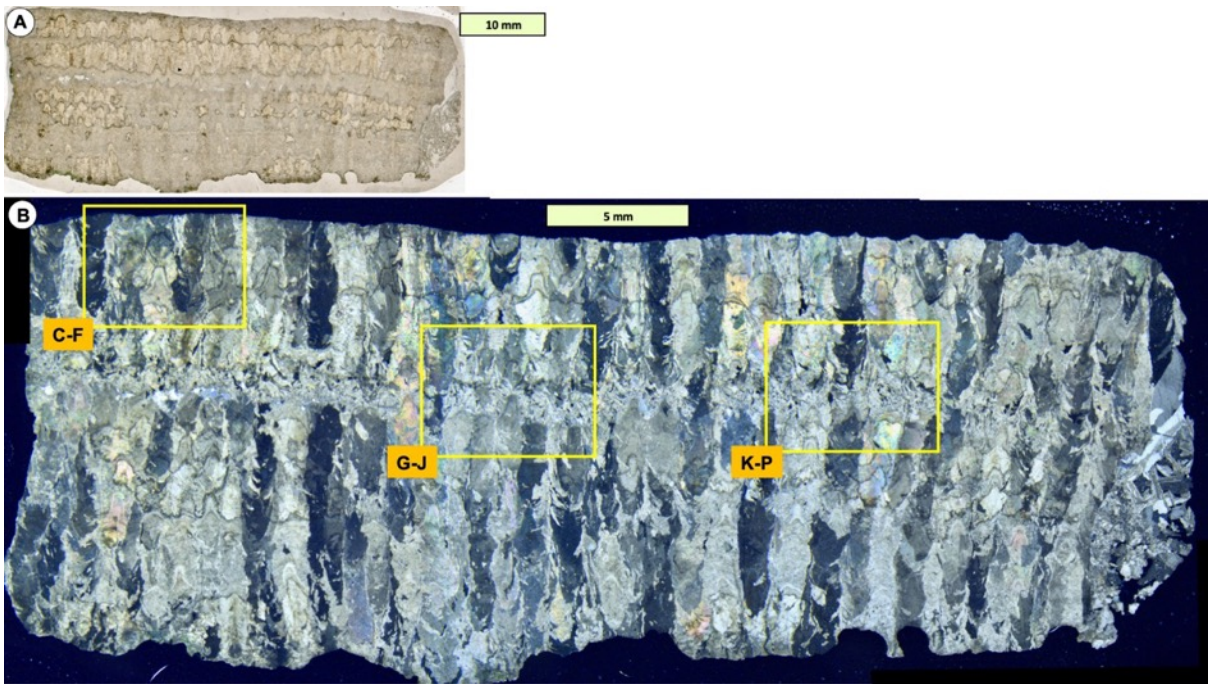

Fig. 6.10-2A-B. VS of previous figures, within the same sample, showing the prominent overprinting of interpreted aggrading neomorphic cystals extending throughout the entire thickness of the specimen, but affected by the early vaguely-fibrous calcite, showing that the overprinting of the earliest stage alteration does not in all cases mask its features. File: 17-10-Case10-3c5-9.45-Ls-VS-TS

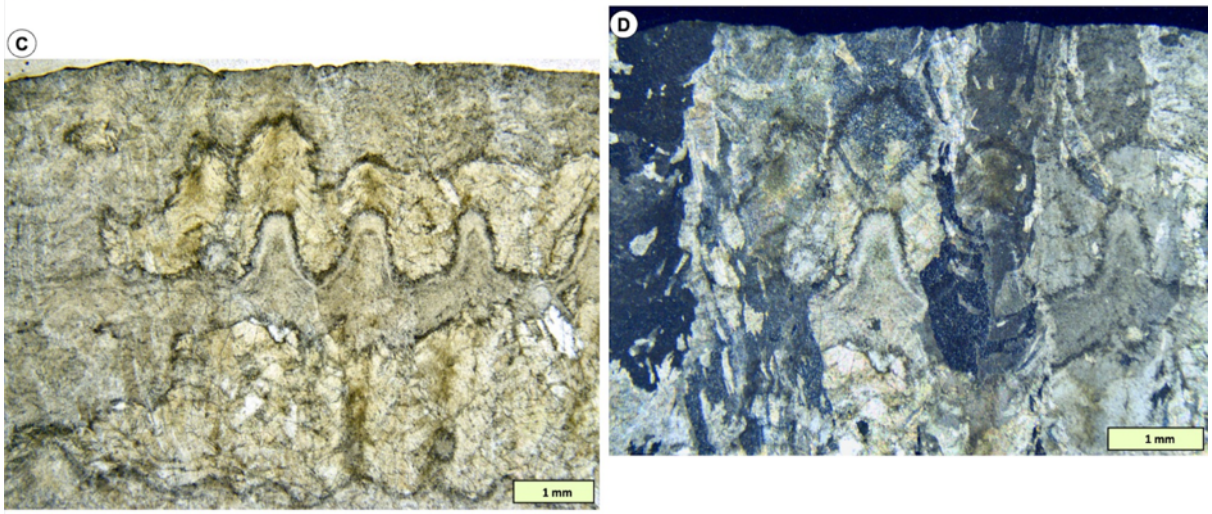

Fig. 6.10-2C-D. Continuation of previous figure showing overprinting of the early-stage vaguely-fibrous calcite by both interpreted stages of 3D crystal fans and the latest interpreted stage of aggrading neomorphic large crystals. Therefore the vaguely-fibrous calcite is the earliest stage of diagenesis in *Ls*; it is also not seen in other stromatoporoids, neither in the Hemse biostromes nor in other deposits with or without *Ls*. File: 17-11-Case10-3c5-9.45-Ls-VS-TS-Cut

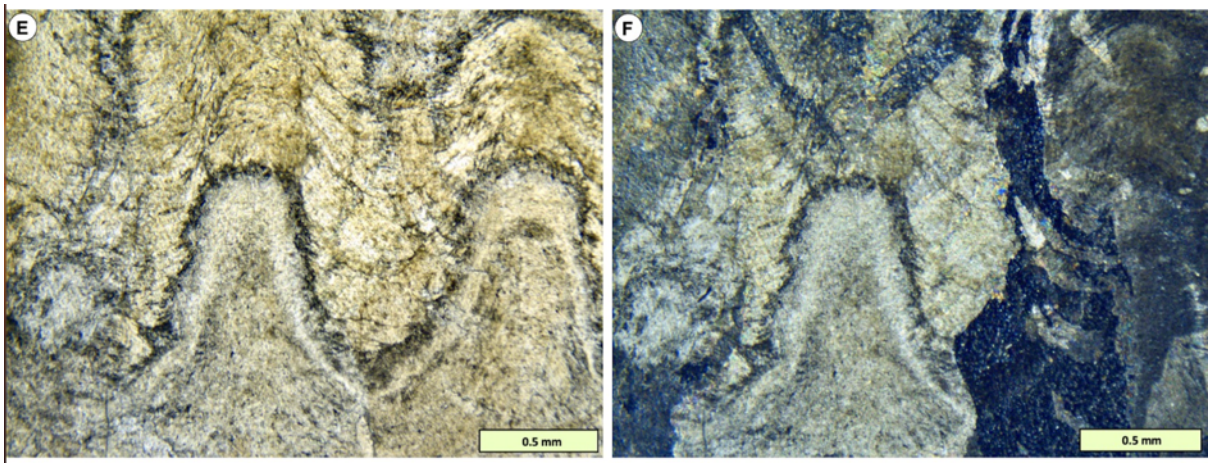

Fig. 6.10-2E-F. Details of previous figure; in the PPL view the vague fibrous calcite fibrosity is clearly visible, overprinted by both the 3D crystal fans and the later aggrading neomorphic change. File: 17-12-Case10-3c5-9.45-Ls-VS-TS-Cut

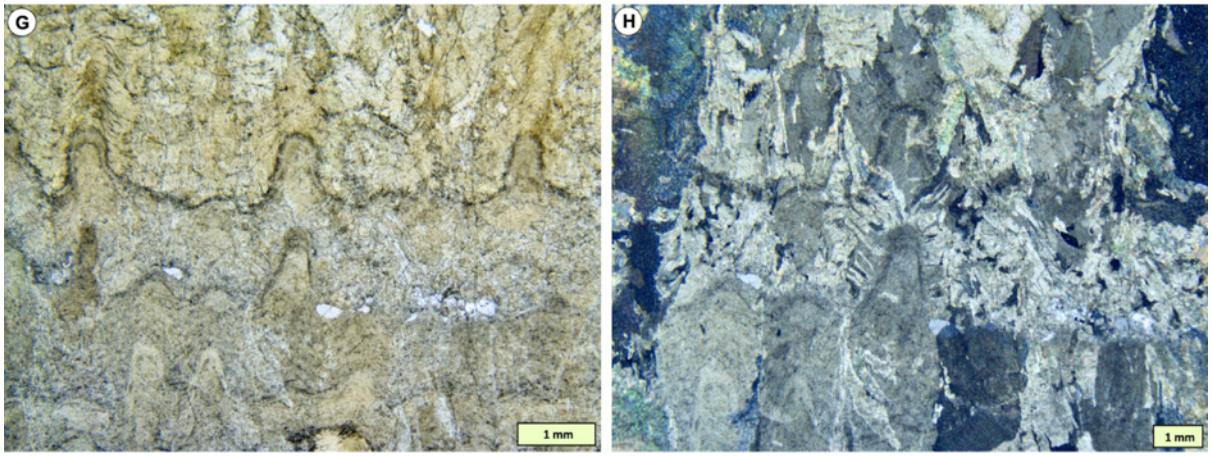

Fig. 6.10-2G-H. More views of interaction between vaguely-fibrous calcite and later diagenetic overprinting. File: 17-13-Case10-3c5-9.45-Ls-VS-TS-Cut

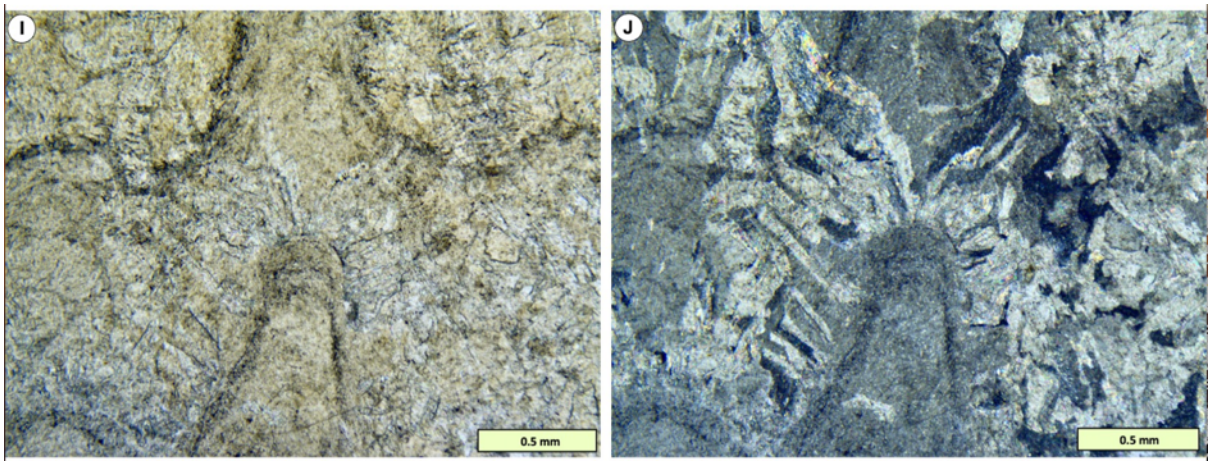

Fig. 6.10-2I-J. Details of previous figure. File: 17-14-Case10-3c5-9.45-Ls-VS-TS-Cut

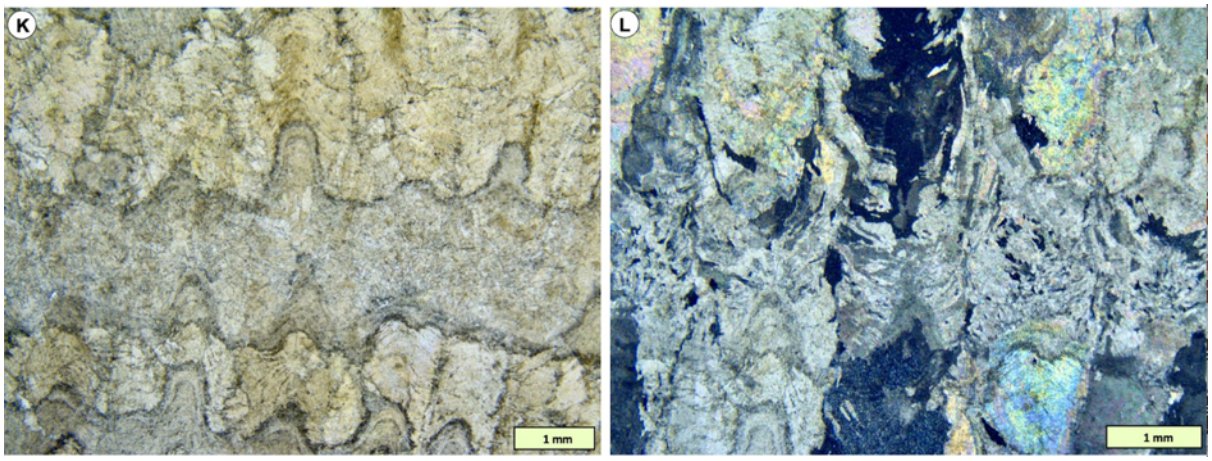

Fig. 6.10-2K-L. More views of interactions of growth features and all three diagenetic overprints. File: 17-15-Case10-3c5-9.45-Ls-VS-TS-Cut

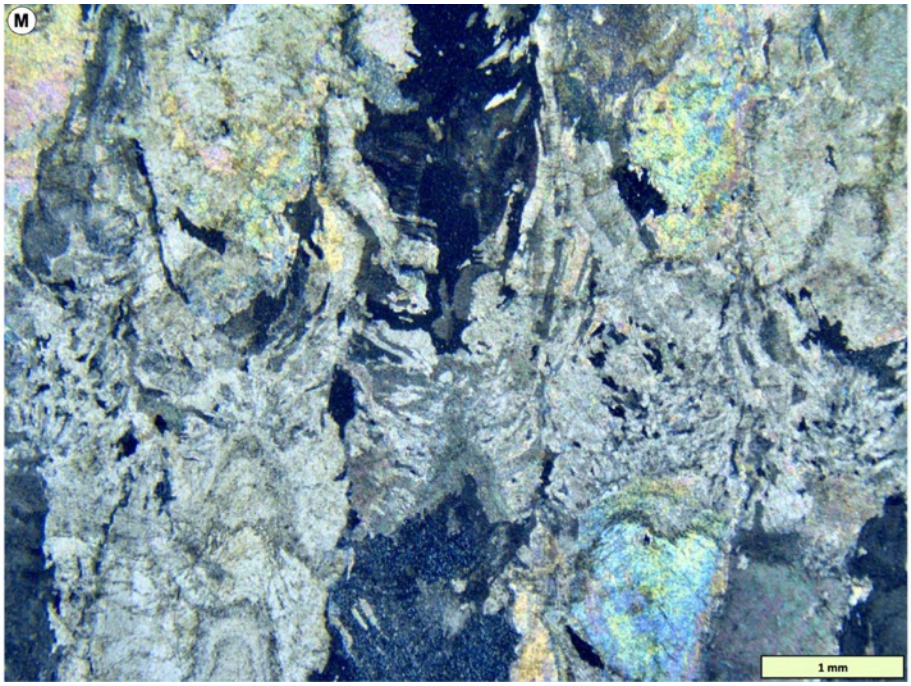

Fig. 6.10-2M. Enlargement of XPL of previous figure showing the three forms of diagenesis in rather beautiful detail. File: 17-16-Case10-3c5-9.45-Ls-VS-TS

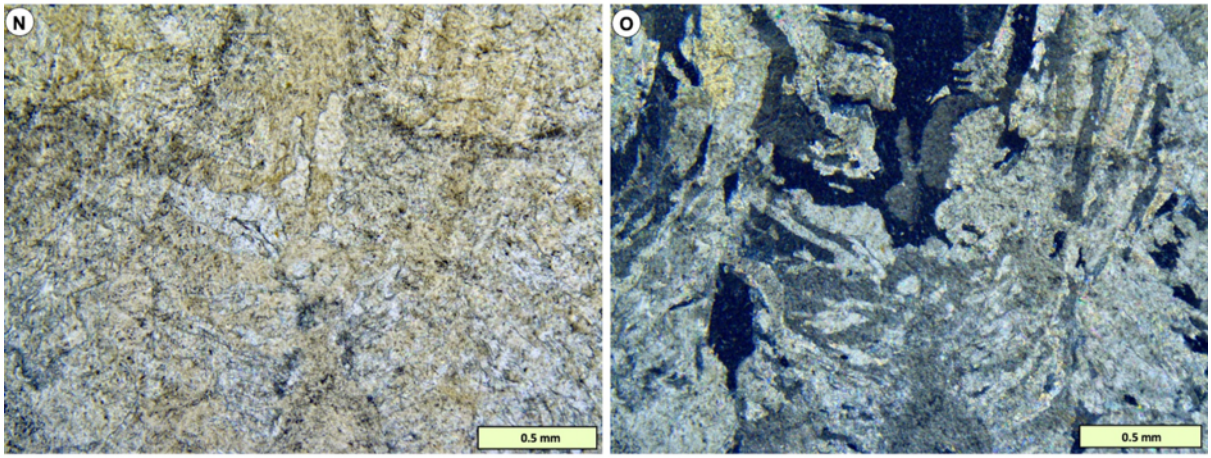

Fig. 6.10-2N-O. High-resolution image of centre of XPL view of previous figure; shows a combination of crystal fans and overprinting aggrading neomorphic calcite. File: 17-17-Case10-3c5-9.45-Ls-VS-TS-Cut

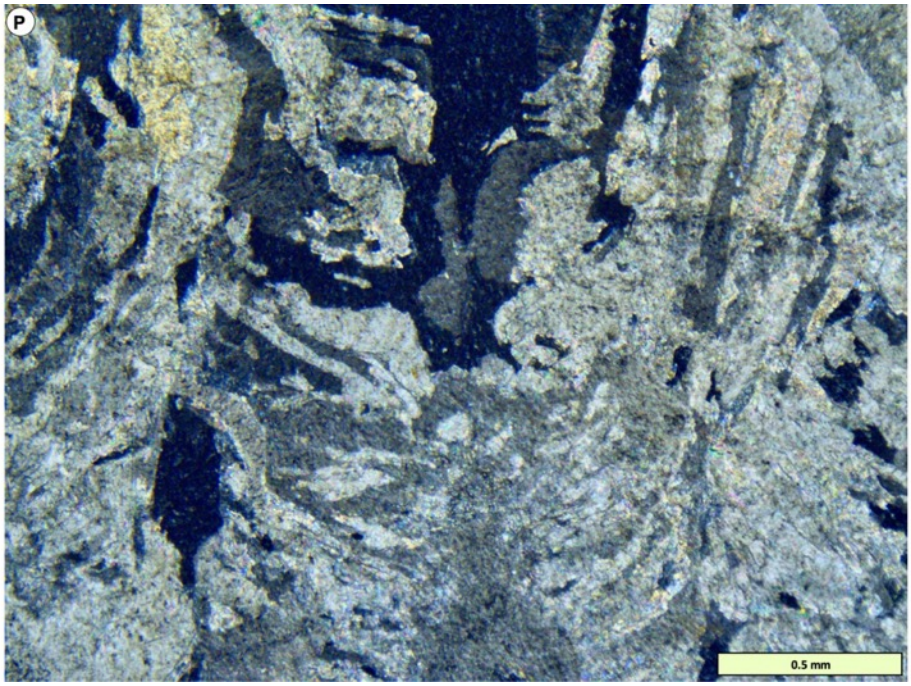

Fig. 6.10-2P. Super-high resolution XPL showing the complex detail of diagenetic overprinting of *Ls*.
File: 17-18-Case10-3c5-9.45-Ls-VS-TS

6.11. Case Study 11: 3b1-5.19

A sample similar to Case 10, included to show variations that exist between individual samples in the same beds. From Kuppen 3, central part of lower biostrome at Kuppen; that is a short distance above the previous Case 10. Thus, Cases 10 and 11 demonstrate the individuality of stromatoporoid diagenesis; they have overall similarity but in individuals there are differences in the precise expression of the diagenetic changes.

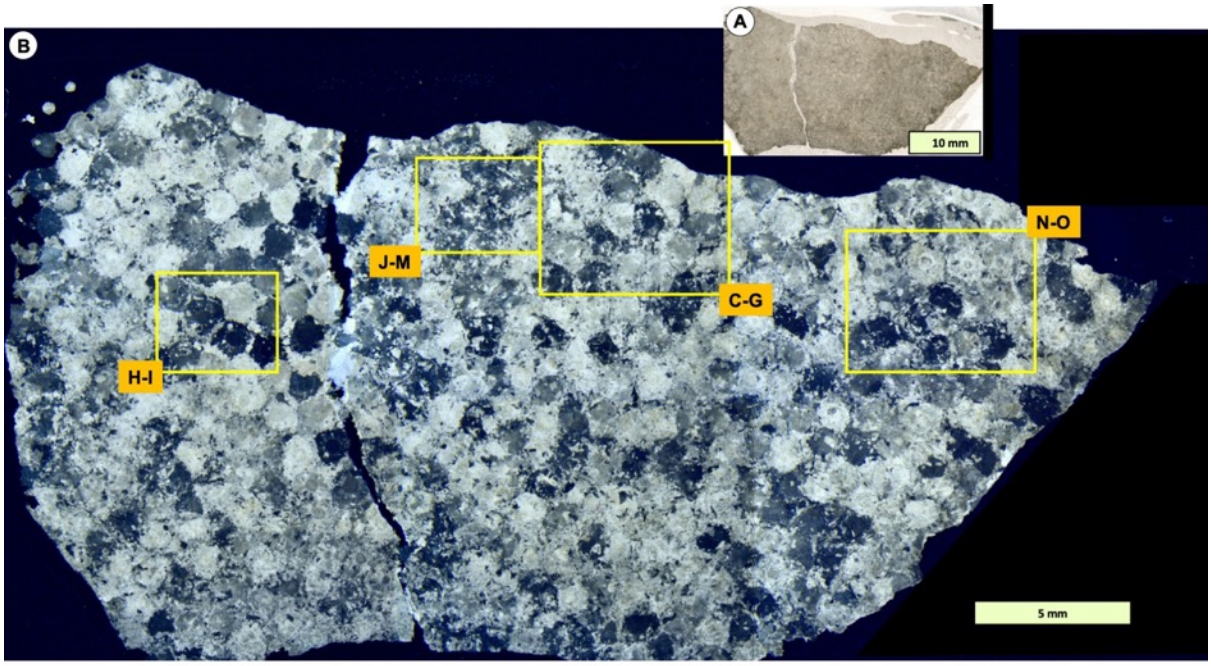

Fig. 6.11-1A-B. TS whole thin section showing variation of alteration explored in detail in following figures. File: 18-01-Case11-3b1-5.19-Ls-VS-TS

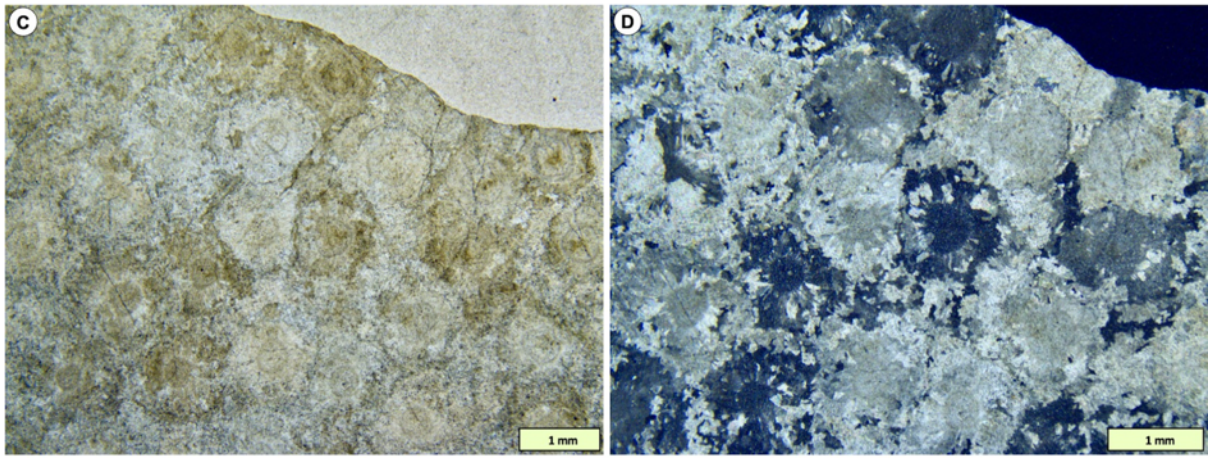

Fig. 6.11-1C-D. TS of *Ls* showing variations of diagenesis across this field of view. File: 18-02-Case11-3b1-5.19-Ls-VS-TS-Cut

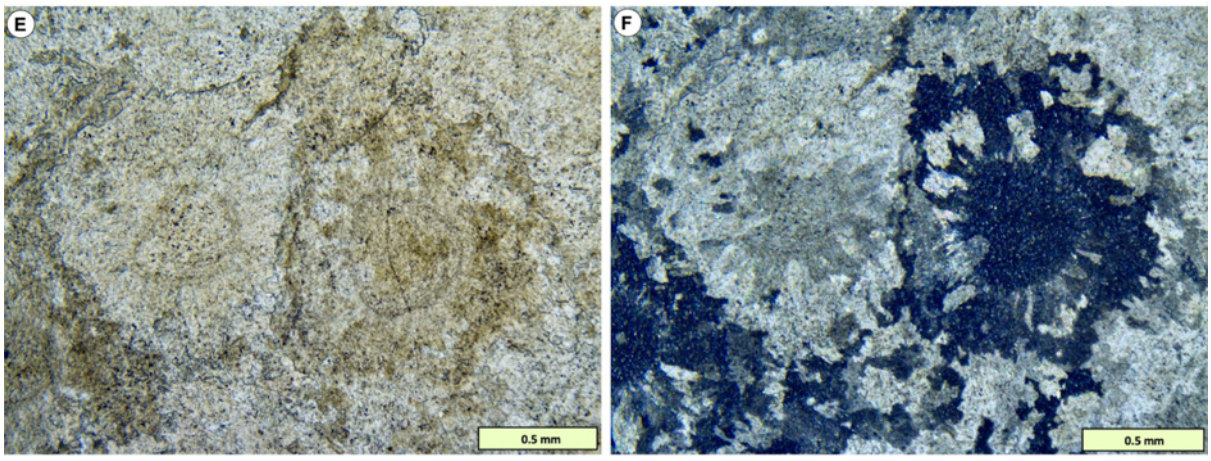

Fig. 6.11-1E-F. Detail of TS showing radial crystals that are interpreted here as being in the process of aggrading neomorphism. ***File: 18-03-Case11-3b1-5.19-Ls-VS-TS-Cut***

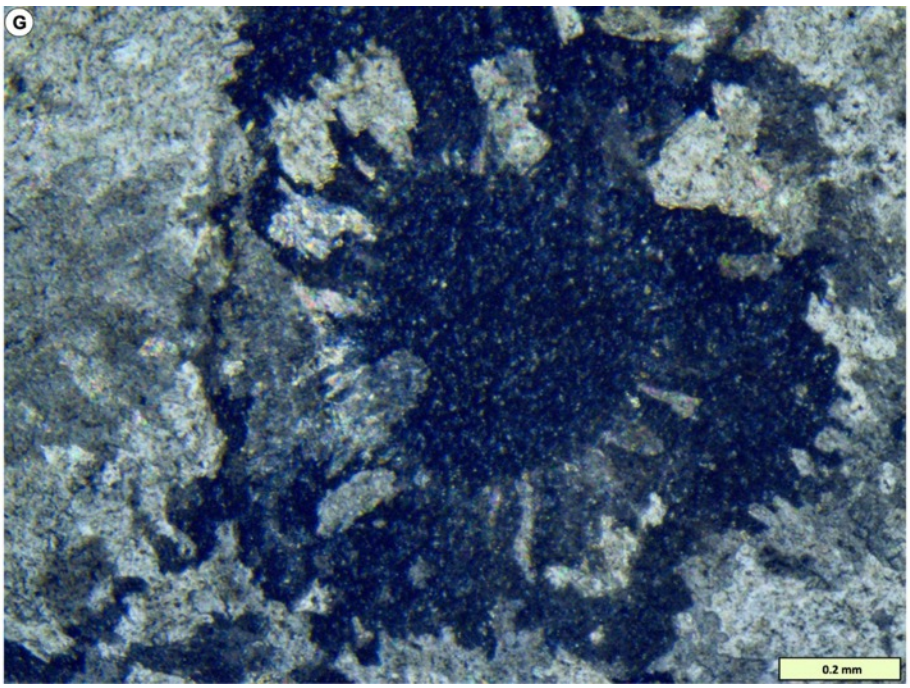

Fig. 6.11-1G. Further detail of previous figure. File: 18-04-Case11-3b1-5.19-Ls-VS-TS

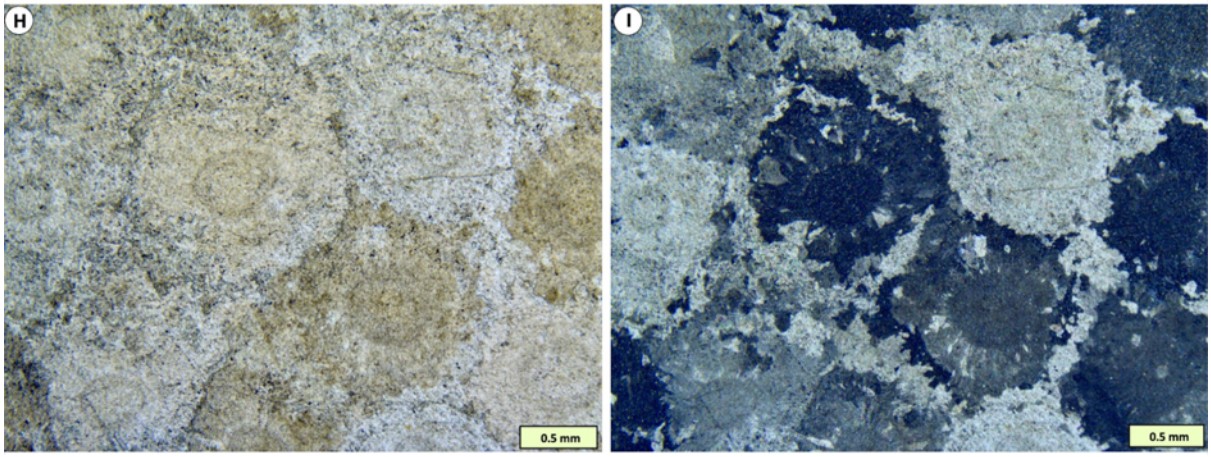

Fig. 6.11-1H-I. More photos of variation of diagenesis in this sample of *Ls.* File: 18-05-Case11-3b1-5.19-Ls-VS-TS-Cut

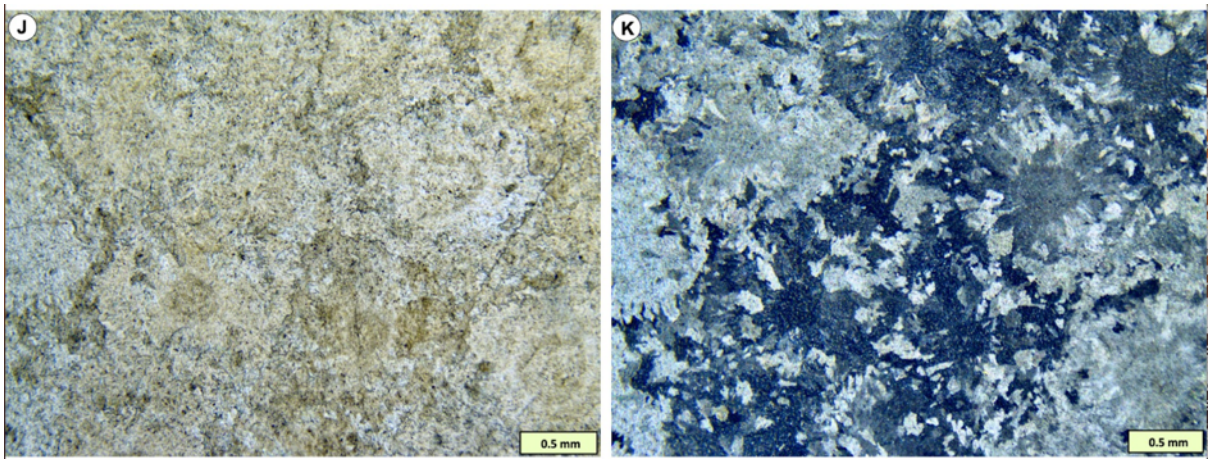

Fig. 6.11-1J-K. Details showing the radial calcite crystals largely disappear in a scattering of crystals, interpreted as the early stage of development to aggrading neomorphism. File: 18-06-Case11-3b1-5.19-Ls-VS-TS-Cut

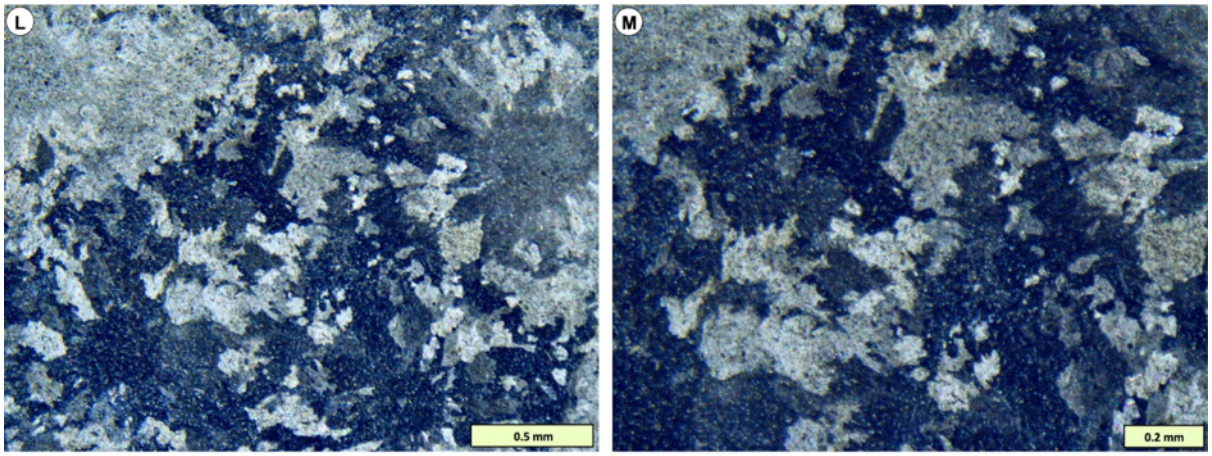

Fig. 6.11-1L-M. More details of previous figure. File: 18-07-Case11-3b1-5.19-Ls-VS-TS-Cut

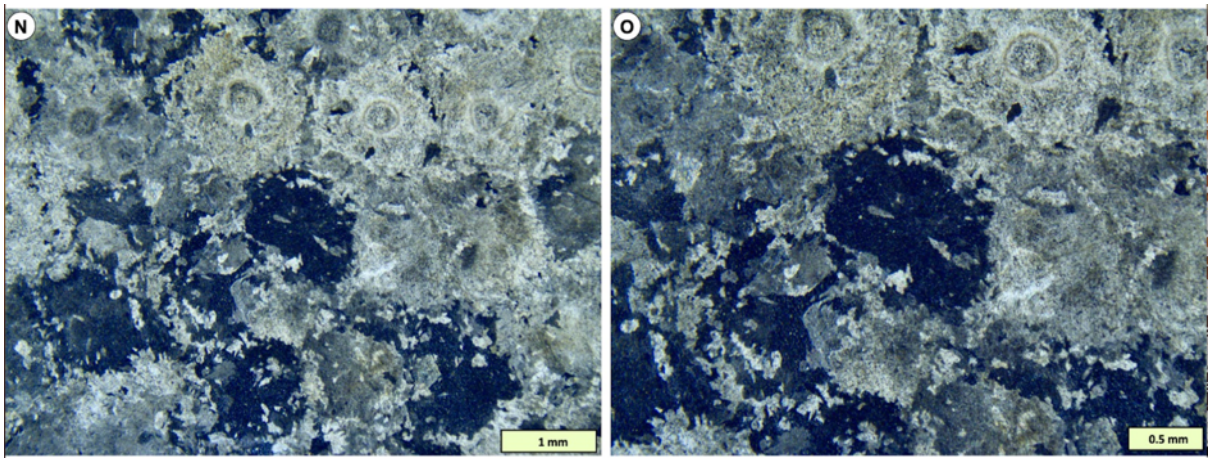

Fig. 6.11-1N-O. Similar views to previous figures. File: 18-08-Case11-3b1-5.19-Ls-VS-TS-Cut

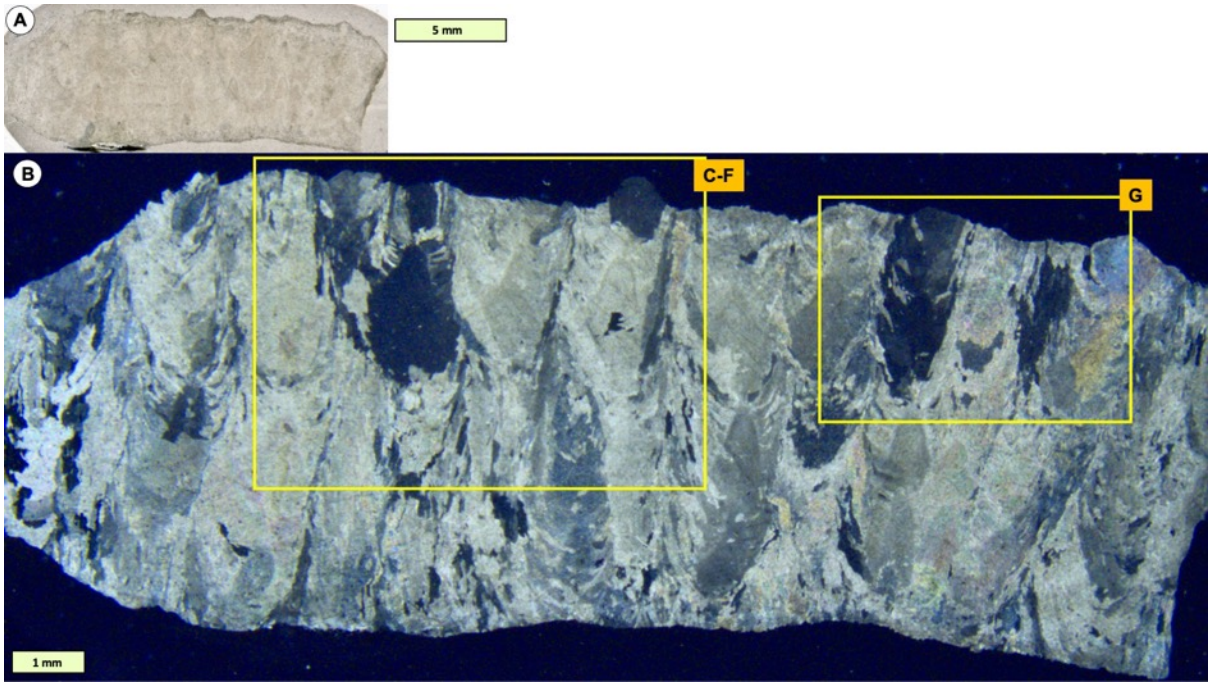

Fig. 6.11-2A-B. VS of same sample as previous figures in this case study showing both 3D radial crystals and interpreted aggrading neomorphic overprinting. File: 18-09-Case11-3b1-5.19-Ls-VS-TS

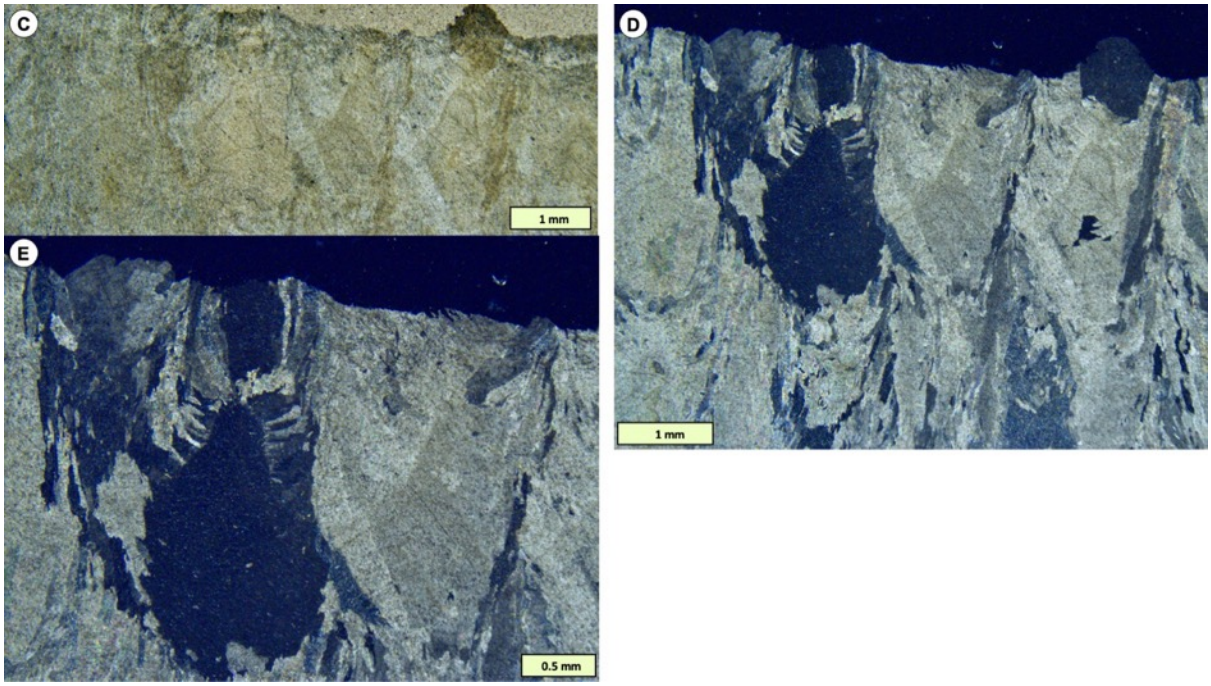

Fig. 6.11-2C-E. Details of previous figure, showing radial calcite and neomorphic aggradation. File: 18-10-Case11-3b1-5.19-Ls-VS-TS

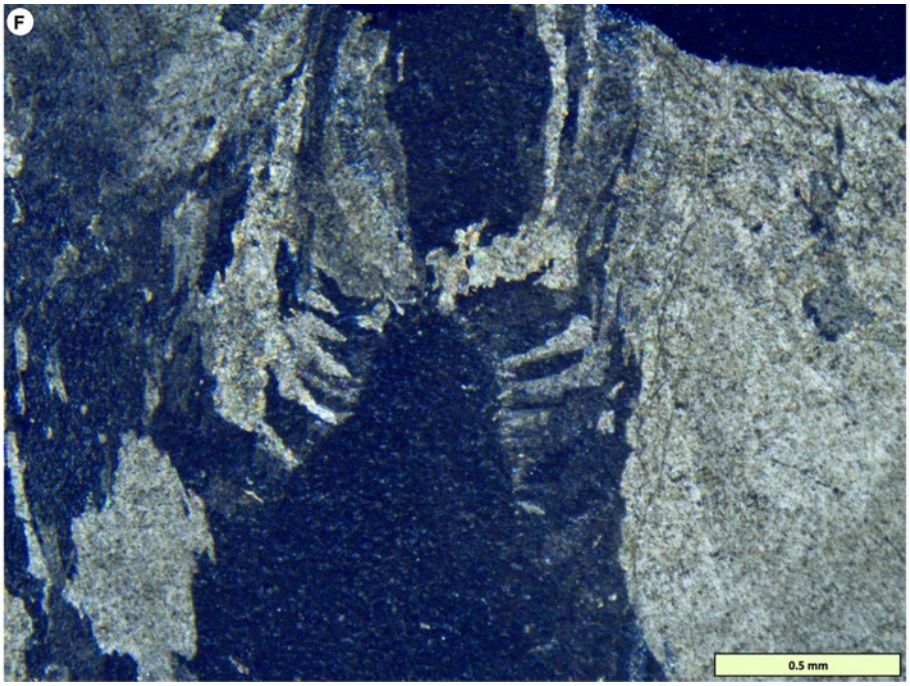

Fig. 6.11-2F. Enlargement of previous figure showing details of the two styles of overprinting in XPL (radial crystal fans and interpreted aggrading neomorphism). ***File: 18-11-Case11-3b1-5.19-Ls-VS-TS***

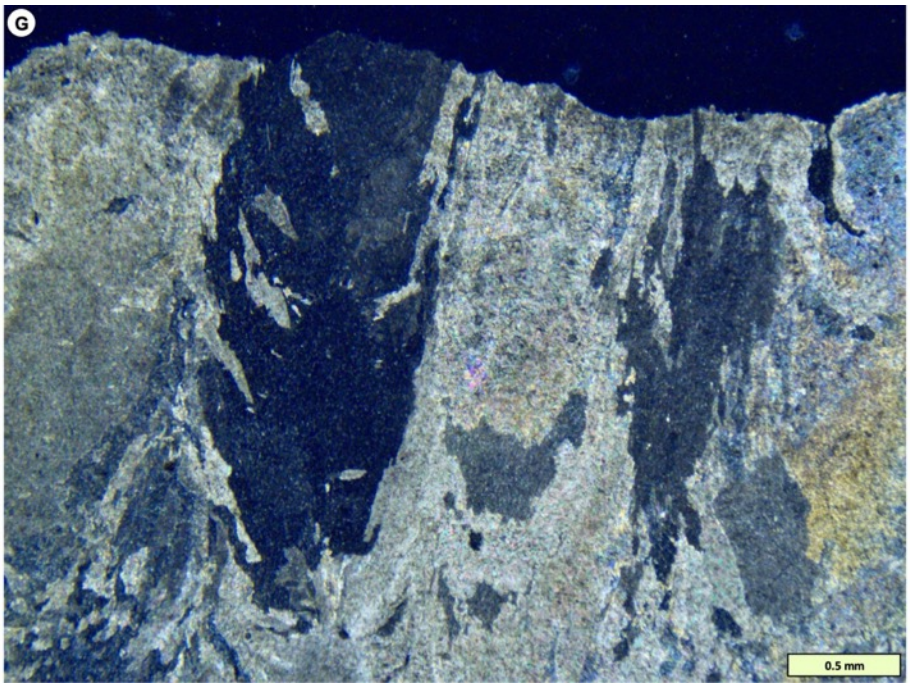

Fig. 6.11-2G. More details of previous figures. File: 18-12-Case11-3b1-5.19-Ls-VS-TS

6.12. Case Study 12: 1a4-3.15

This sample is from Kuppen 1 locality near the top of the biostrome, a short distance below the erosion surface at the top of the lower biostrome. This sample shows contiguous crystals with irregular compromise boundaries and is interpreted to represent the latest stage of diagenetic change, that is near the end of the interpreted aggrading neomorphic process.

However the VS shows the base of the stromatoporoid in contact with calcareous mudstone that it is presumed to have grown over, and shows the diagenetic alteration does not extend into the underlying sediment. This sample is therefore another demonstration that the diagenesis of *Ls* is contained within its structure, that is a characteristic of all stromatoporoids.

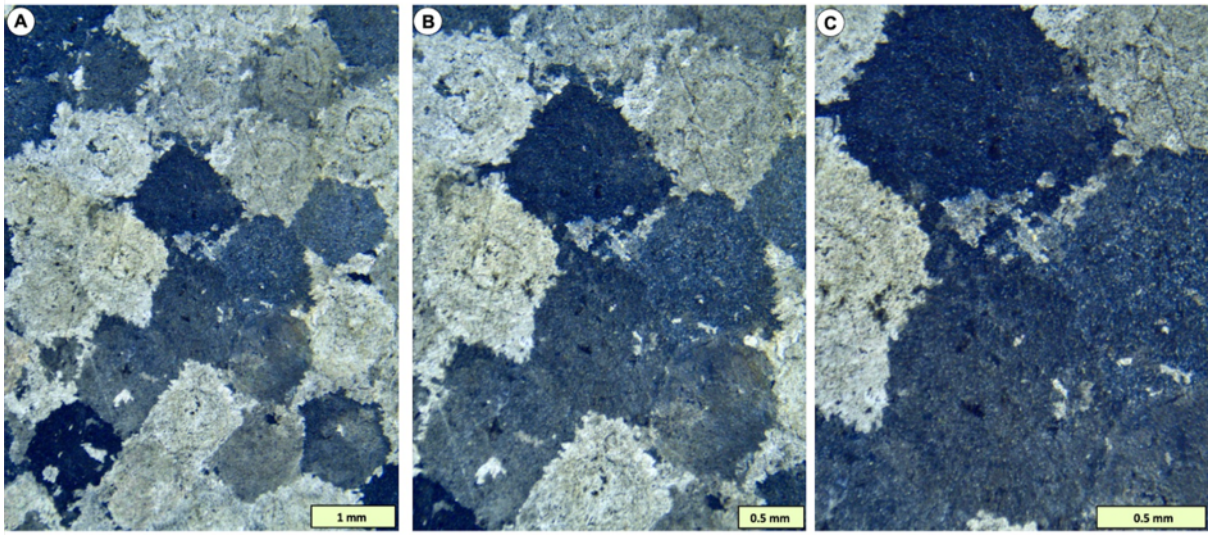

Fig. 6.12-1A-C. TS showing the irregular contiguous compromise boundaries of interpreted aggrading neomorphic crystals centred on the tightly upcurved features of which *Ls* is principally constructed. File: 19-1-Case12-1a4-3.15-Ls-VS-TS-Cut

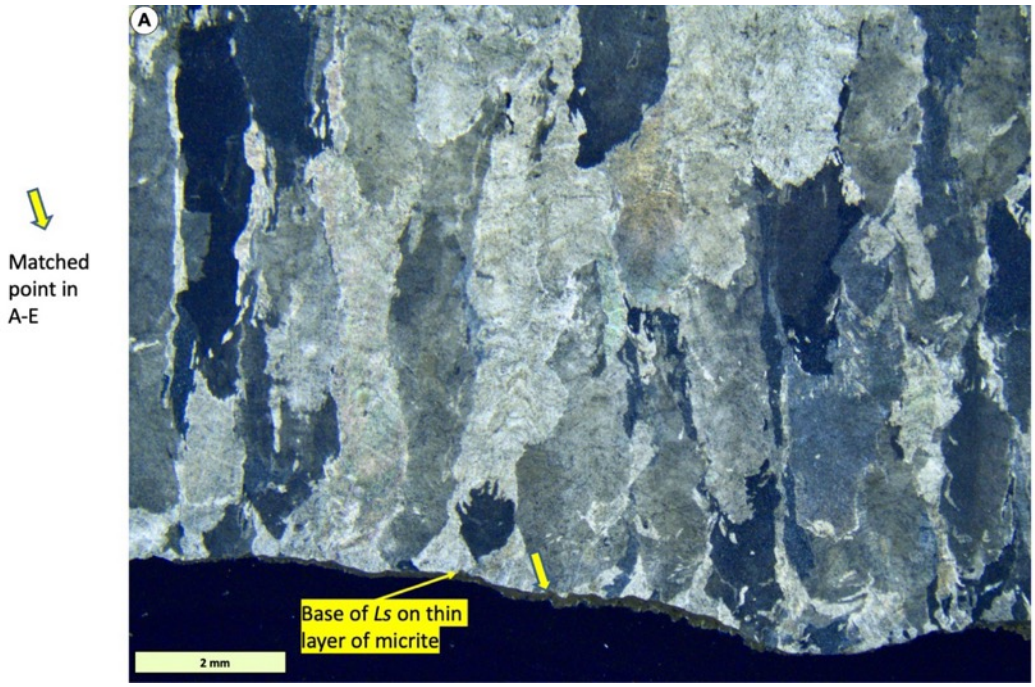

Fig. 6.12-2A. VS Overview of *Ls* on sediment base. Note the diagenesis stops sharply at the base of the stromatoporoid and does not pass into the underlying sediment. File: 19-2-Case12-1a4-3.15-Ls-VS-TS

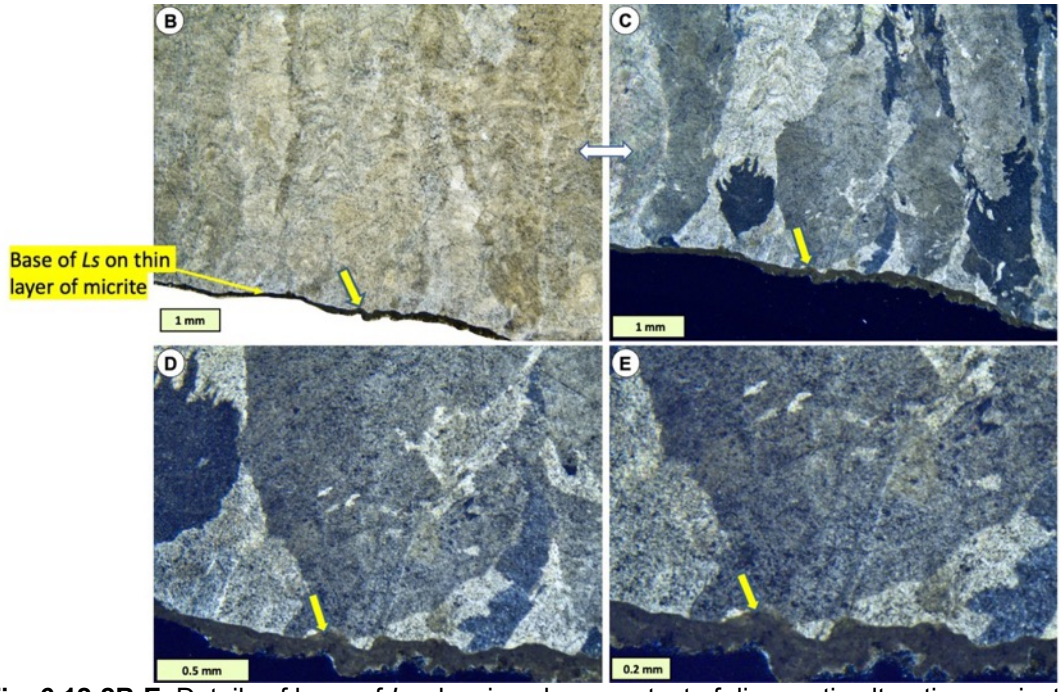

Fig. 6.12-2B-E. Details of base of *Ls* showing sharp contact of diagenetic alteration against the sediment that the stromatoporoid is presumed to have grown on. File: 19-3-Case12-1a4-3.15-Ls-VS-TS

6.13. Case Study 13: 3c3-3.94

Cement filling of a fracture in the *Ls.* This fracture is interpreted to have been open when the stromatoporoid was diagenetically altered, so indicates either: 1) that the fracture may have developed during a storm by the stromatoporoid being in sharp collision with other objects (likely other stromatoporoid skeletons) on the sea bed; Or 2) that the laminar structure of this particular stromatoporoid taxon was liable to break under shallow burial but the fracture remained open until the stromatoporoid was recrystallised. Note that Kershaw et al. (2021, Facies paper) interpreted stromatoporoid diagenesis to have been generally an early process, in shallow burial; so a combination of environmental violent collision and shallow burial fracturing under load can explain the formation of these fractures.

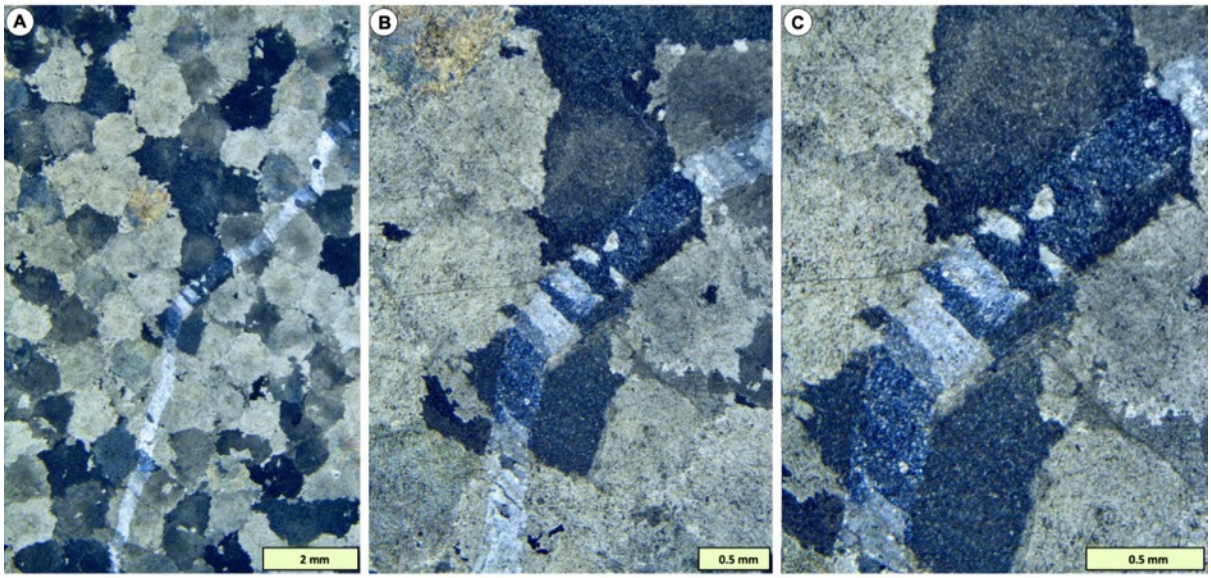

Fig. 6.13. TS views in XPL at different scales of a cement-filled fracture in the skeleton, that contains cement in optical continuity with the crystals of the diagenetically altered skeleton. This is interpreted to indicate that the cement filling of the fracture did not take place until the skeleton of *Ls* was altered. If instead the fracture was cemented before the recrystallisation of the *Ls* occurred then there would be expected to be a sharp contact between the cement of the fracture and the cement of the altered *Ls*. File: 20-Case13-3c3-3.94-Ls-TS

6.14. Case Study 14: KLoose54-iii-Stained

Stromatoporoids stained with a combined stain of Alizarin Red S and potassium ferricyanide (ARS-KFeCN) generally show that the skeleton is red-stained, therefore non-ferroan calcite, while gallery space may or may not contain blue cement, therefore ferroan calcite, that is formed below the redox boundary in shallow burial diagenesis. The images here show *Ls*, *Ps* and *Pc*, demonstrating that all three taxa have non-ferroan skeletons. This adds to the overall view that alteration of stromatoporoids in diagenesis was an early process in their diagenetic history.

However, these pictures show an additional feature, that is of unstained patches in the structure. In these rather thick sections the structure of these unstained patches is not clear, but subsequent to these pictures being taken, further thinning of the thin section revealed that the unstained patches have a yellow colour in XPL that indicates quartz in a still-slightly-thick section. Silicification of stromatoporoids is common and in this case shows that the skeletal structure is more silicified than the galleries. Kershaw et al. (2021, Facies paper) go into more detail of the silicification process and show that cases vary; in some examples the skeleton is preferentially silicified; in others the gallery cements are preferentially silicified; in yet others, ALL of it is silicified. It may depend on time, so that if enough time is allowed the entire structure of skeletons and cements become silicified. The images presented here do show variation of silicification of skeleton and gallery cement.

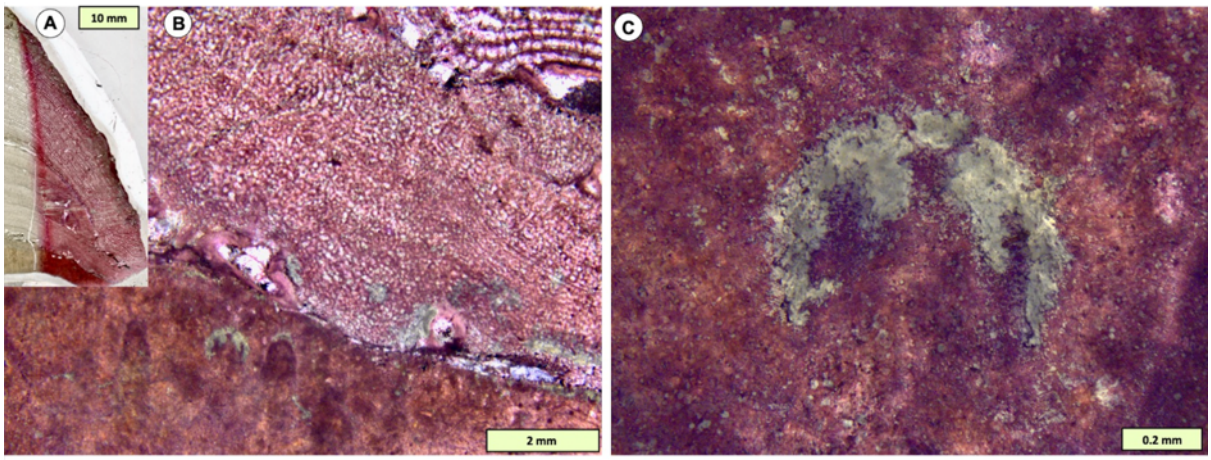

Fig. 6.14-1. VS of a stacked sample of *Ls* at the base, encrusted by *Ps*, then *Pc*. C shows enlargement of lower centre of the lower stromatoporoid *Ls*, the crescent-shaped unstained area matches the shape of one of the tight upcurved pillar-like features of which *Ls* is constructed. Thus the silicification follows the curved structure. File: 21-1-Case14-KLoose54-iii-Stained-Cut

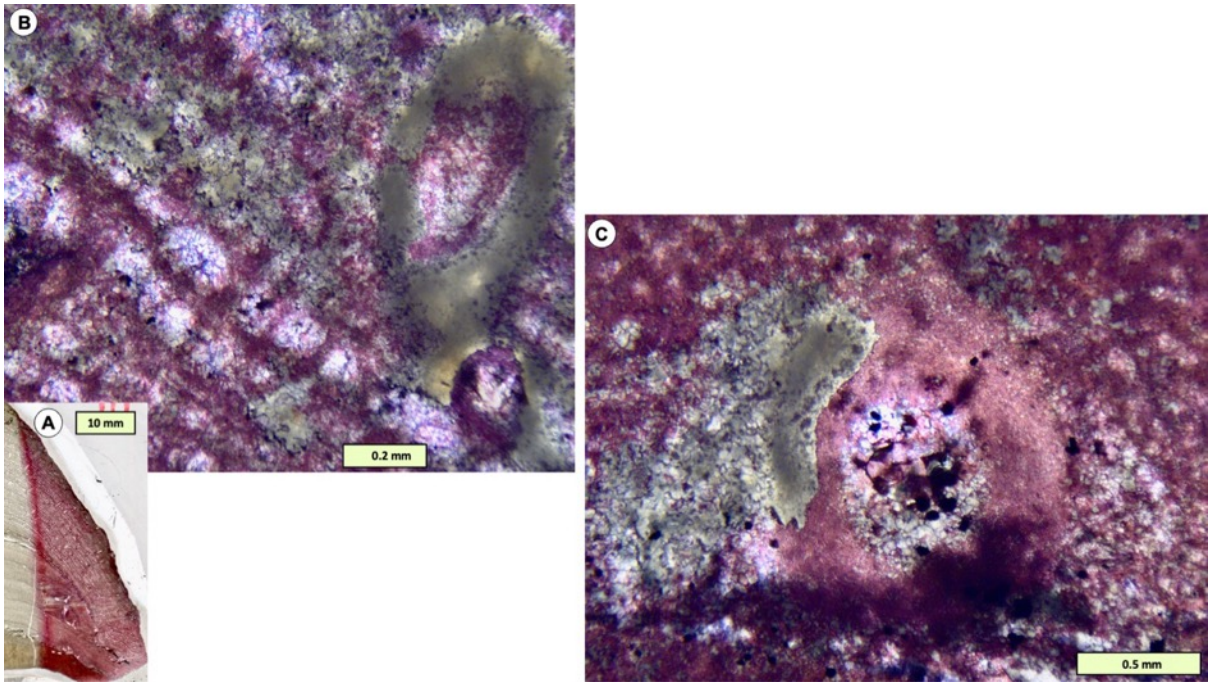

Fig. 6.14-2. B. PPL VS, enlargement of the upper part of the stromatoporoid stack, of *Pc*, that has intergrown syringoporid tabulate tubes within the laminae-pillar architecture of the *Pc.* This photo shows the entire cross section of the intergrown syringoporid is silicified, but the stromatoporoid is only partly altered, with both skeleton and gallery cement partly affected by the alteration. **C.** is located at the contact between *Ls* and *Pc*; the darker area at the bottom of the picture is the very top layer of *Ls*. Encrusting the top surface of the *Ls* is an auloporid tube in TS and that tube is encrusted by *Ps.* Note that the auloporid tube is partially silicified and that silicification affects the *Ps* skeleton next to the auloporid. In the upper centre-right of the photo are small patches of unstained *Ps* reflecting a scatter of silicification affecting both the skeleton and gallery space of the Ps. File: 21-2-Case14-KLoose54-iii-Stained

SECTION 7:
Lophiostroma schmidtii structural and diagenetic model

The diagram in Fig. 7.1 shows a schematic reconstruction of *Lophiostroma schmidtii*, combining the range of information presented in this atlas. The diagram is divided into 4 stages of development, from 1-4, left to right. Stage 1 is the growth model, substantially based on CL imagers; Stages 2-4 show diagenetic change of three types, progressing from left to right. See caption for more details.

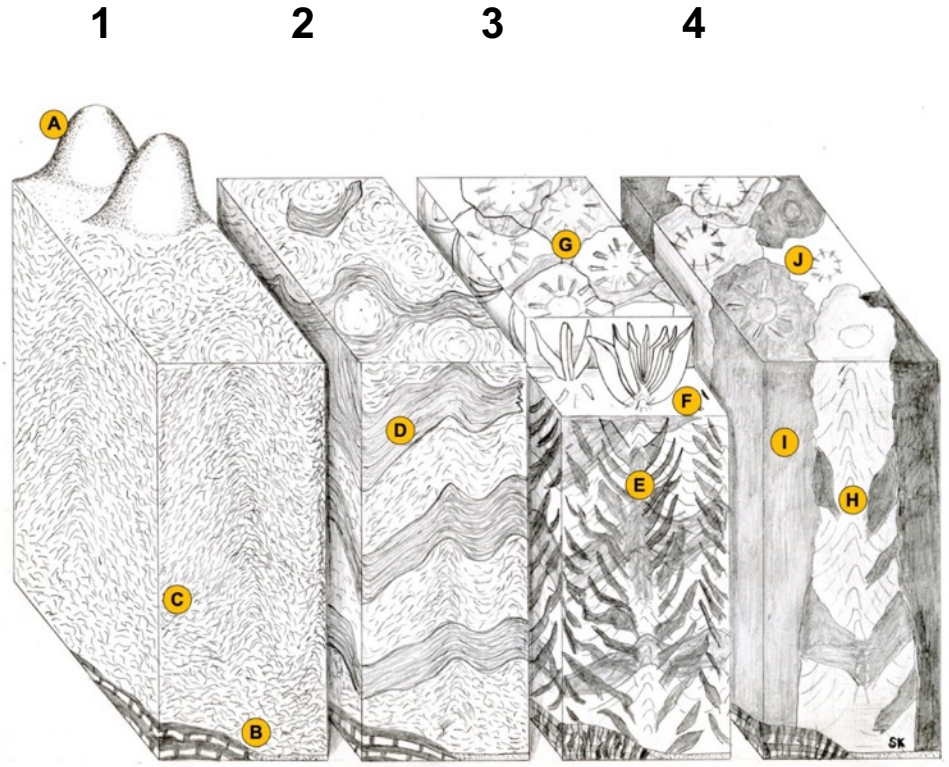

Fig. 7.1. 3D reconstruction drawing of *Lophiostroma schmidtii* (*Ls*). The diagram is divided into 4 Stages, that occur chronologically from left to right. Each block of the diagram is about 2 mm wide.
Stage 1: growth reconstruction. A. Surface of *Ls* shows papillae as typical features, that represent the upper surface terminations of the upcurved laminations. The front 2/3 of this top surface represent a TS cut through the structure. **B.** Base of *Ls* grew partly on another stromatoporoid (left) and sediment (right). **C.** Schematic reconstruction of layering in *Ls* showing the stacked small irregular plates where the upcurved parts are synchronous, forming stacks that look like vertical pillar-like structures, but are actually made of stack coinciding plates. This structure is best seen in CL, on which this part of the diagram is based.
Stages 2-4: diagenetic sequence, illustrated in XPL.
Stage 2: D. XPL reconstruction of overprinting of growth layers by vaguely-fibrous calcite, that developed along the curved structure of *Ls*. The nature of this overprinting is not clear; it is not known in other stromatoporoids in the same or different beds and appears to be a feature unique to *Ls*
Stage 3: E & F. XPL reconstruction of overprinting of laminar structure of *Ls* by a fabric-retentive system of 3D upwardly-expanding crystal fans that grow at high angles to the orientation of the laminations, thus form these fans in response to the 3-dimensional geometry of the wavy nature of the skeletons lamination.. F shows a small area of simplistic 3D drawing of the crystal fans. **G.** The diagenetic overprinting began to develop compromise boundaries between areas centred on the upward curving stacked laminations, indicating the entire structure is undergoing alteration and reorganisation.
Stage 4: H. Seen in XPL, the 3D crystal fans undergo aggrading neomorphism to form larger crystals, that in some places retain the crystal fan arrangement, as around H, but in other places (I) only single

crystals remain. **J.** the TS view shows some of the crystal fans are still represented within the single crystals of stage 4, but others have lost the crystal fans because of interpreted aggradation to single crystals.

SECTION 8:
Comparative stromatoporoid taxa

In this section are four stromatoporoids illustrated that have similarities to *Lophiostroma schmidtii*. Two are from the Silurian of Gotland and the other two are from the Silurian of England. These images are included to show more stromatoporoids of unquestioned stromatoporoid groups, that have similarity of structure to *Ls* and thus aid in the view presented in this atlas that *Ls* is best classified as a stromatoporoid.

8.1. Pachystylostroma visbyense, Lower Visby Fm, uppermost Llandovery, Silurian, Gotland

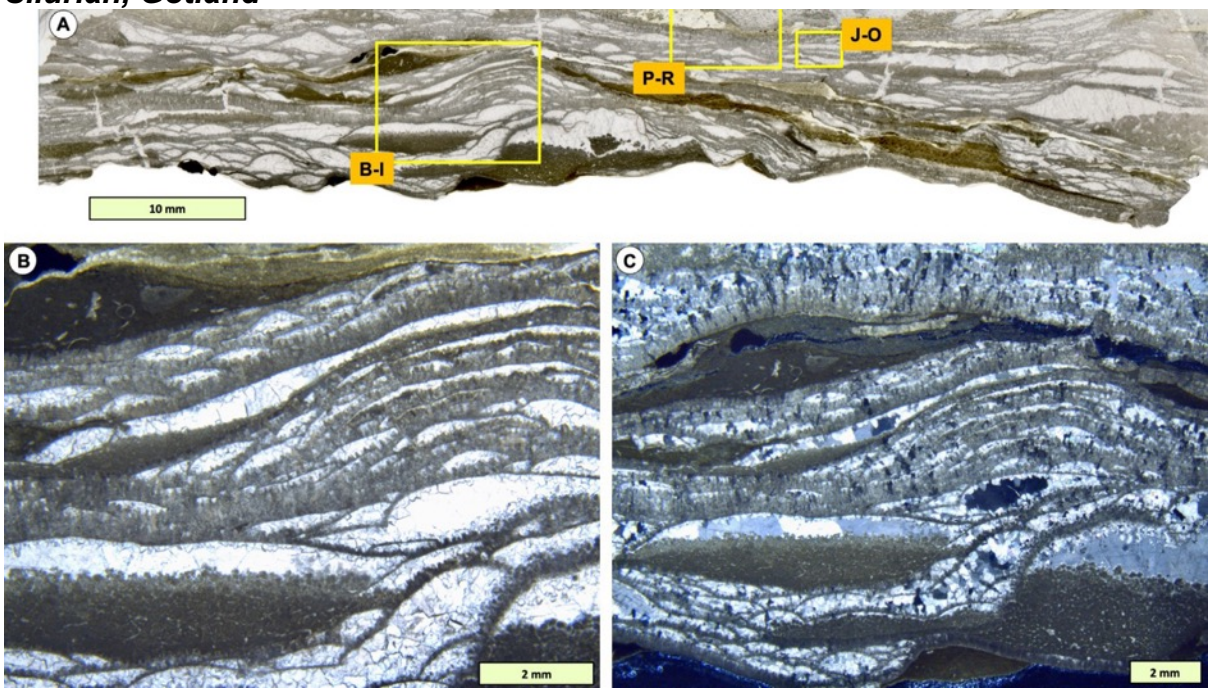

Fig. 8-1A-C. A. VS of whole thin section of *Pachystylostroma* showing its open framework of laminations with plates and geopetal infills. The open spaces cannot be really called galleries, because they are not within the skeletal structure, that instead comprises thin sheets of stromatoporoid skeleton roofing over to form cavities. **B-C.** PPL (B) and XPL (C) enlargements of left-hand box in A showing some details, more in the following figures. File: 23-01-HAK-03-Pachystylostroma

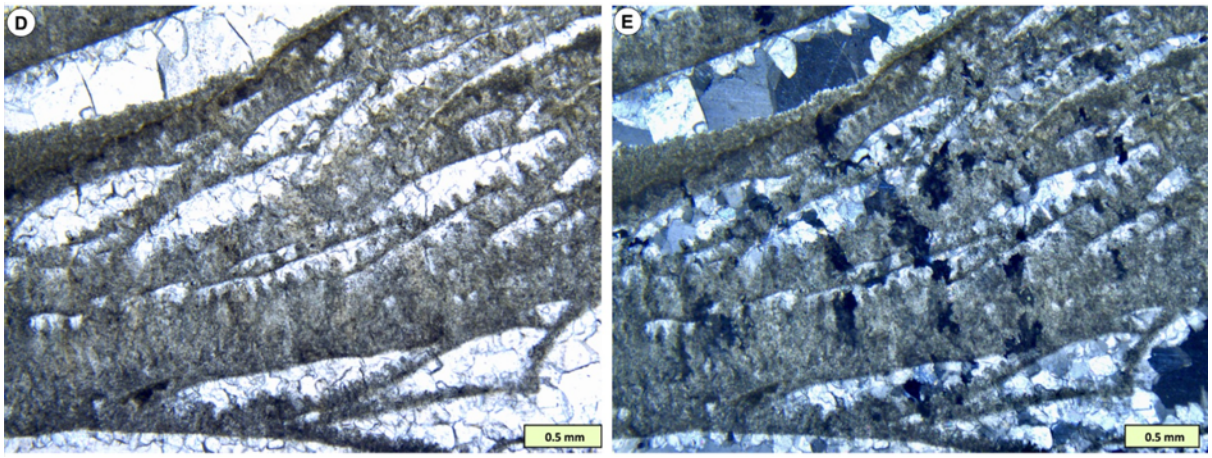

Fig. 8-1D-E. Enlargements of central part of B & C respectively, showing the recrystallisation fabric (FRIC) that cuts across the laminations and in some cases passes into the space between laminations. File: 23-02-HAK-03-Pachystylostroma-Cut

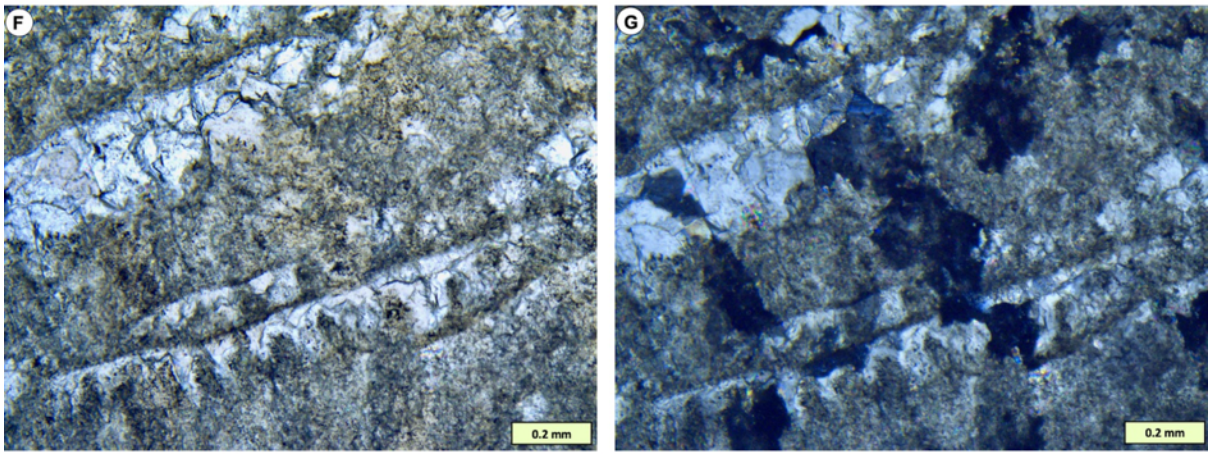

Fig. 8-1F-G. Enlargements of central part of D & E respectively, highlighting the FRIC in G, that occurs in all stromatoporoids, passing into the space between layers. File: 23-03-HAK-03-Pachystylostroma-Cut

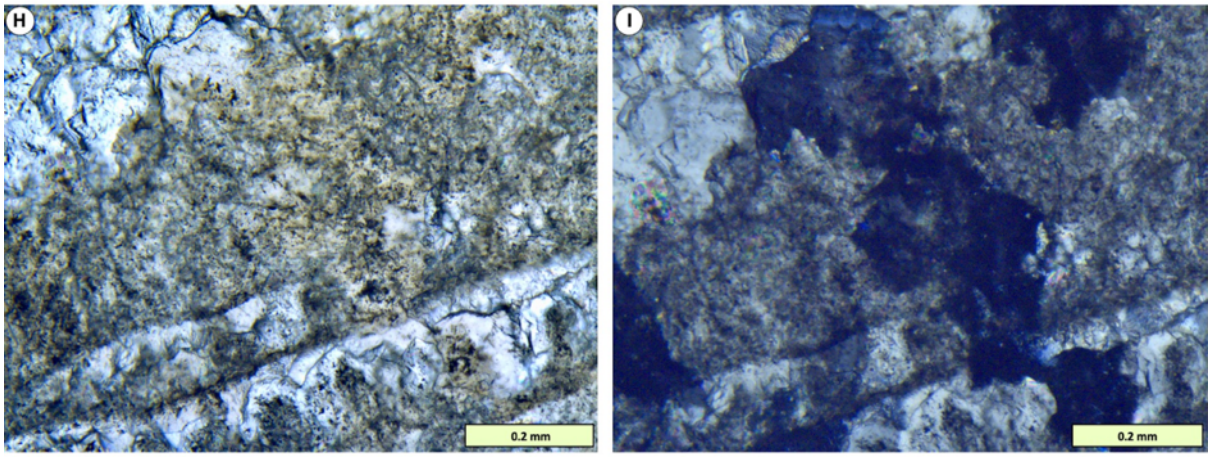

Fig. 8-1H-I. Enlargements of F & G respectively showing highest resolution of details of the skeleton. In PPL (H) the stromatoporoid skeleton looks dense and structureless, the prominent papillae on the uppe surface of each lamination is clearly visible. File: 23-04-HAK-03-Pachystylostroma-Cut

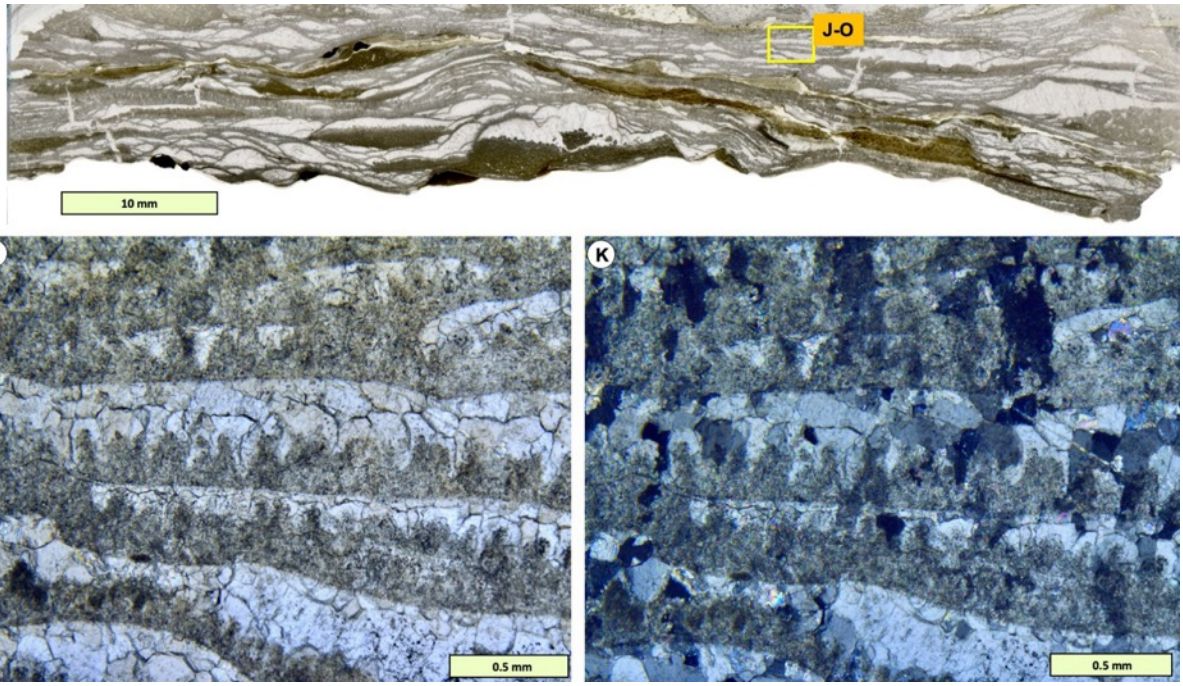

Fig. 8-1J-K. PPL and XPL, showing further details of overprinting of stromatoporoid skeletal structure by diagenetic FRIC that passes into the primary growth cavities, evidence that those cavities were open when the stromatoporoid recrystallised, and thus an indication of early diagenesis in stromatoporoids. This feature is characteristic of all stromatoporoids. File: 23-05-HAK-03-Pachystylostroma

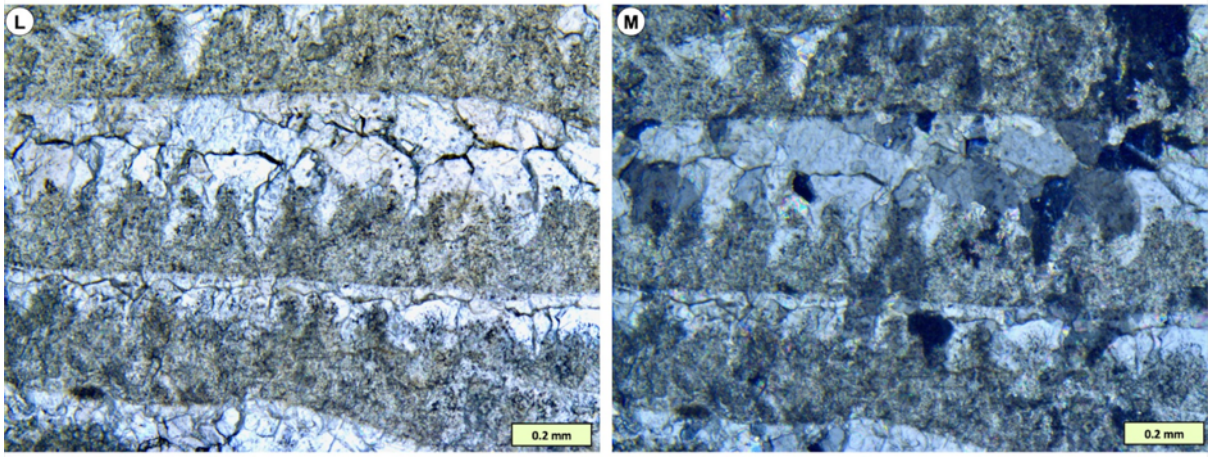

Fig. 8-1L-M. PPL and XPL enlargements of previous figures. File: 23-06-HAK-03-Pachystylostroma-Cut

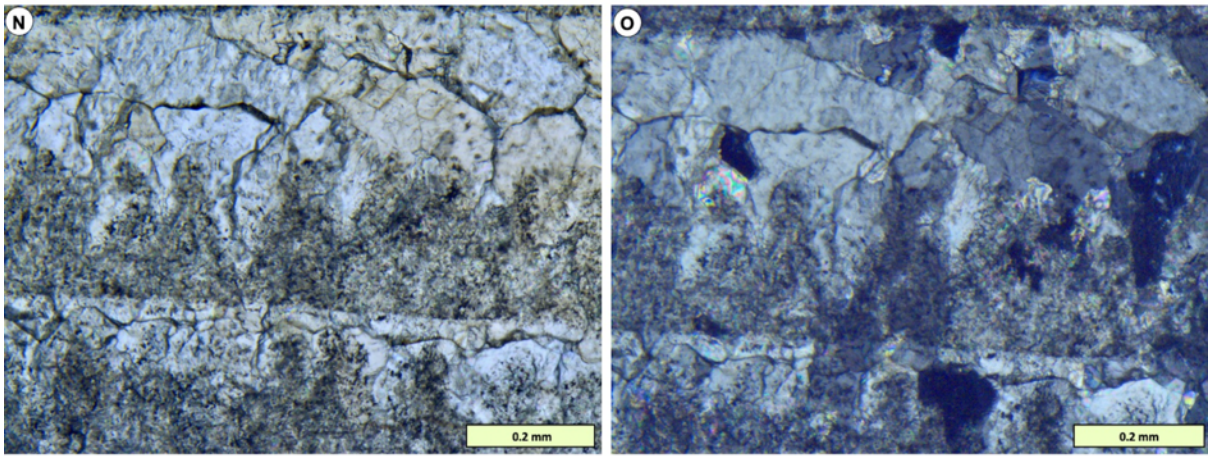

Fig. 8-1N-O. PPL and XPL showing more details of diagenetic overprinting. File: 23-07-HAK-03-Pachystylostroma-Cut

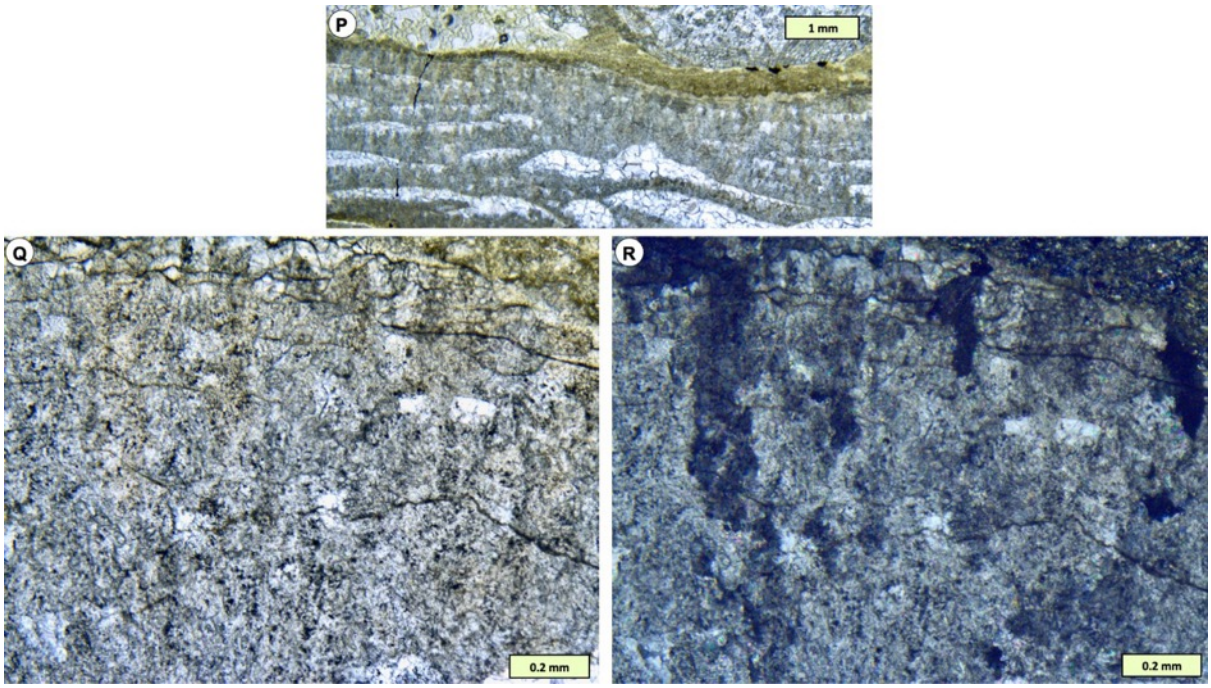

Fig. 8-1P-R. Area of more solid mass of *Pachystylostroma* showing the FRIC passing through its skeletal structure. File: 23-08-HAK-03-Pachystylostroma

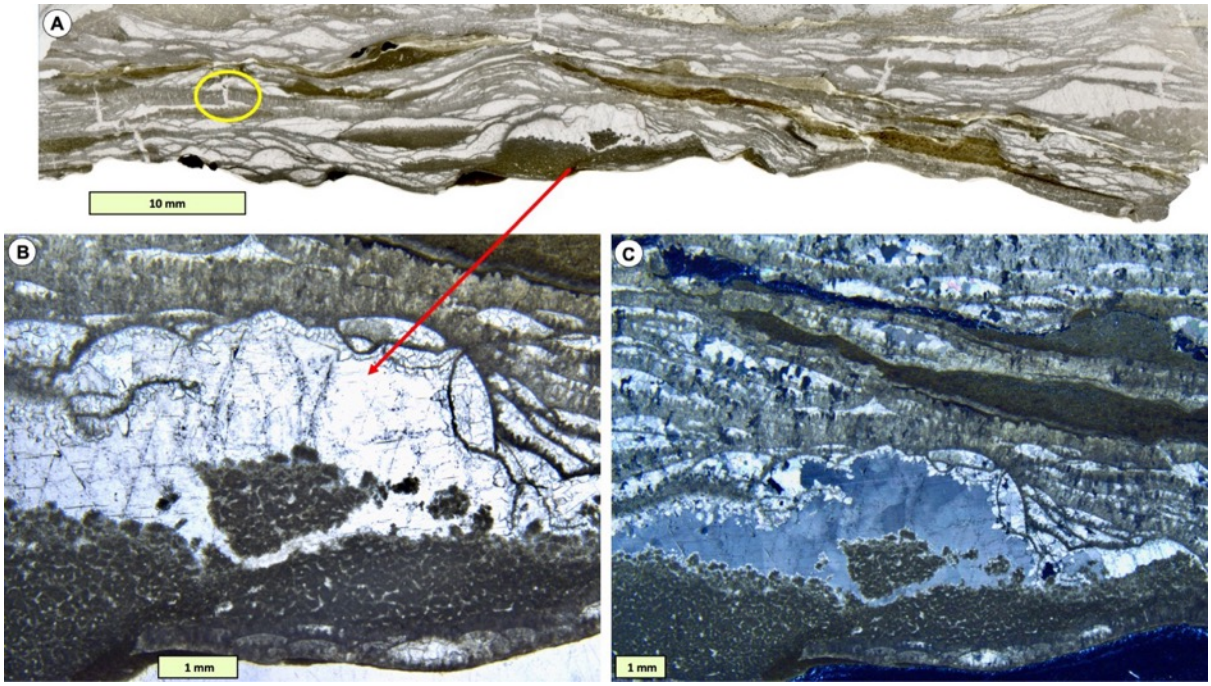

Fig. 8-2A-C. Geopetal near base of stromatoporoid, showing a peculiar feature of a piece of geopetal peloidal fill separated from the main deposit. It is not clear how this happened, but presumably the geopetal peloidal fill was cemented early, then broken, presumably by force (maybe a storm impact while on the sea bed – if true, this indicates the cementation was very early. File: 23-09-HAK-03-Pachystylostroma

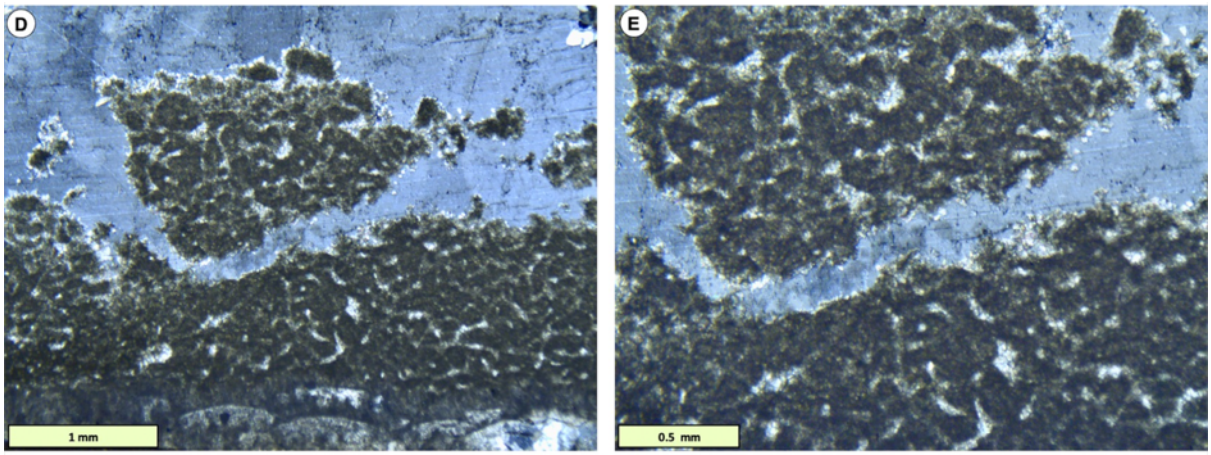

Fig. 8-2D-E. Details of geopetal in previous pictures. File: 23-10-HAK-03-Pachystylostroma-Cut

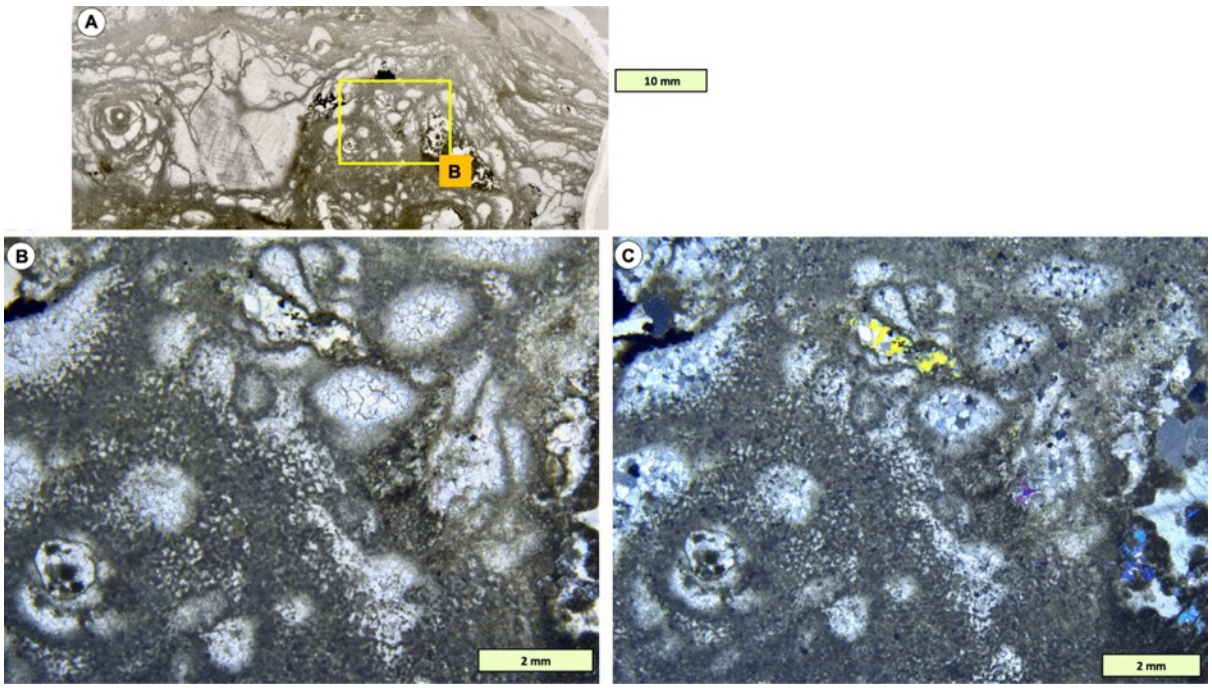

Fig. 8-3A-C. TS of *Pachystylostroma* showing the TS sections through primary cavities and through individual pillar tops. File: 23-11-HAK-03-Pachystylostroma

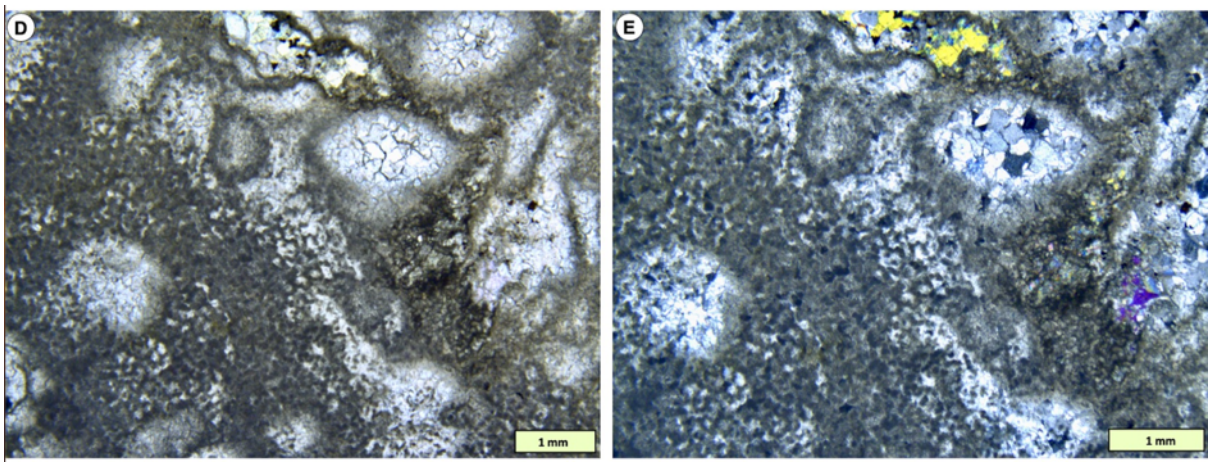

Fig. 8-3D-E. Enlargement of previous figure showing more details of *Pachystylostroma* structure in TS File: 23-12-HAK-03-Pachystylostroma-Cut

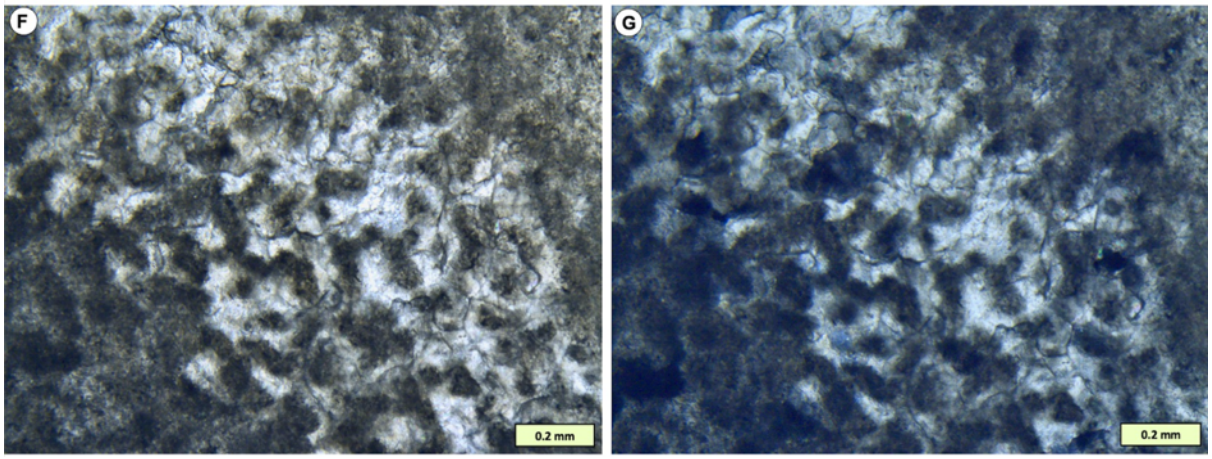

Fig. 8-3F-G. Enlargement of previous figures showing more detail of pillars. File: 23-13-HAK-03-Pachystylostroma-Cut

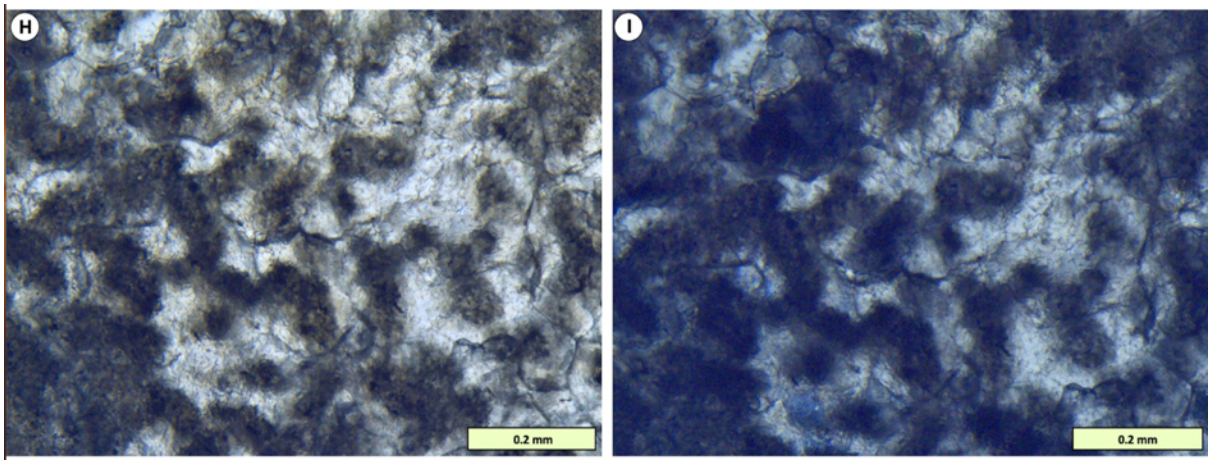

Fig. 8-3H-I. Higher resolution view of pillars, showing their oblong shape and micritic structure, the same as that seen in VS. File: 23-14-HAK-03-Pachystylostroma-Cut

8.2. Pachystroma hesslandi, Upper Visby Fm, lowermost Wenlock, Silurian, Gotland

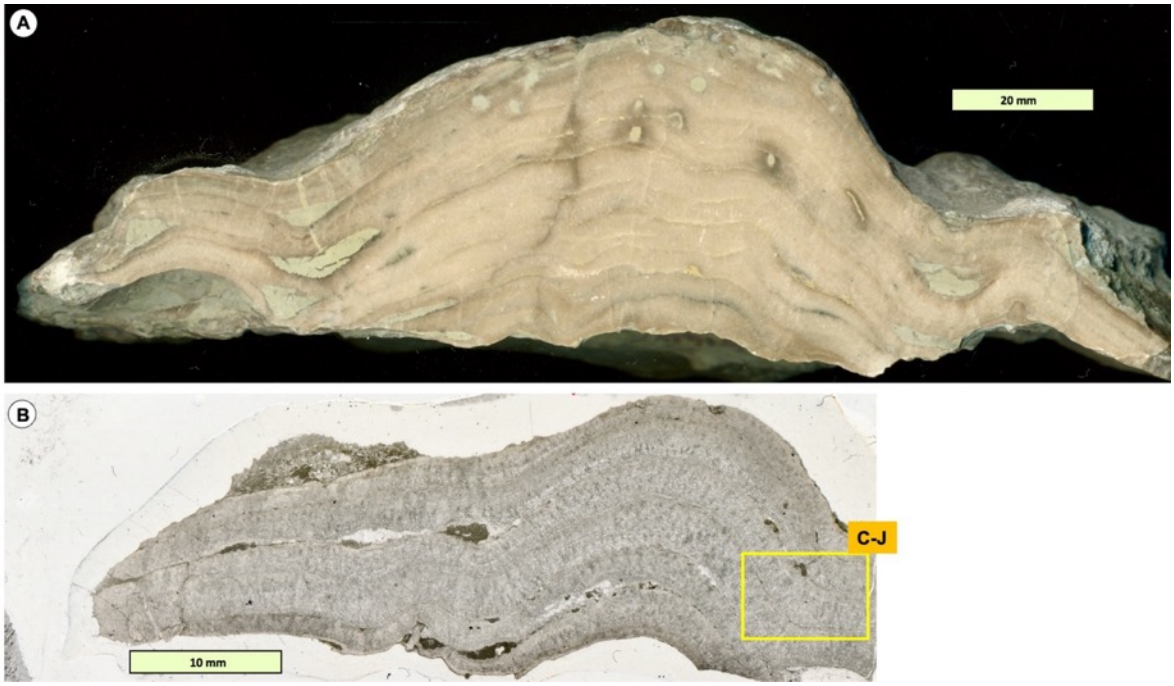

Fig. 8-4A-B. Cut vertical sample (A) and large thin section view (B) of another taxon – *Pachystroma hesslandi* , Upper Visby Formation, lower Wenlock, Gotland, Sweden, for comparison with *Ls* and with *Pachystylostroma.* Note that the old name of *Pachystroma hesslandi* is *Pseudolabechia hesslandi*, a taxon named by Mori (1969) from Gotland. File: 24-01-K-13

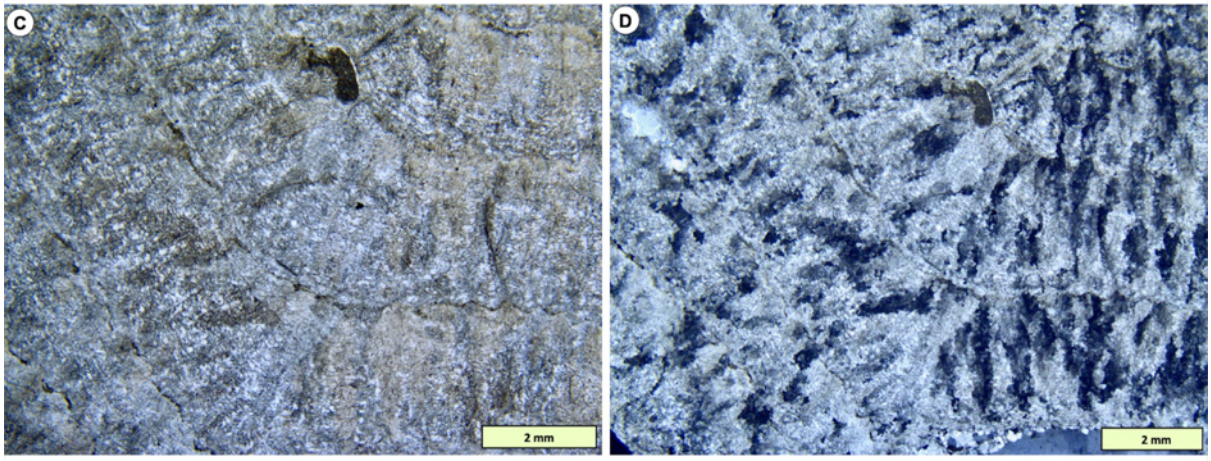

Fig. 8-4C-D. VS details of *Pachystroma hesslandi* in PPL (C) and XPL (D). Note in XPL the overprinting FRIC that is characteristic of all stromatoporoids. File: 24-02-K-13-Cut

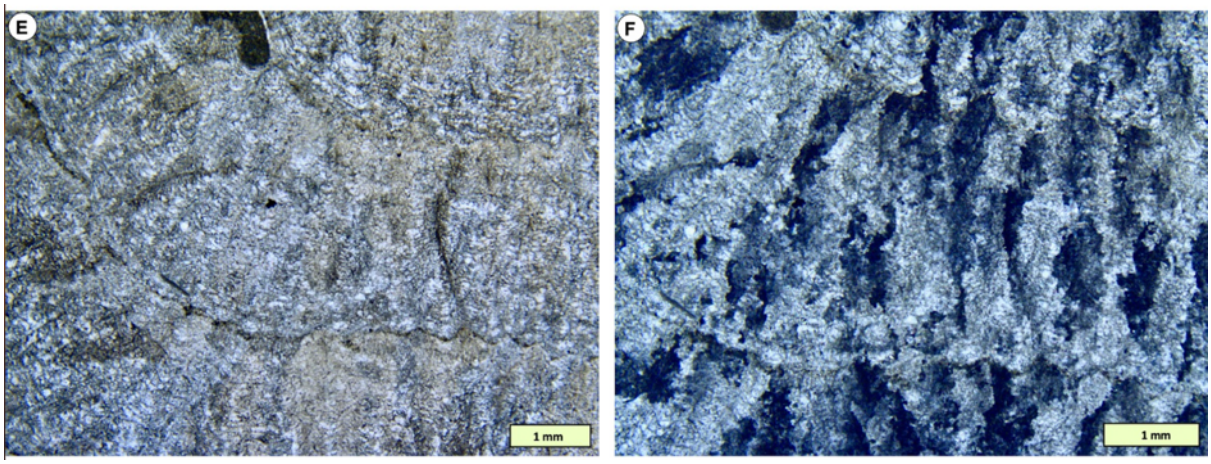

Fig. 8-4E-F. Detail of PPL and XPL views. File: 24-03-K-13-Cut

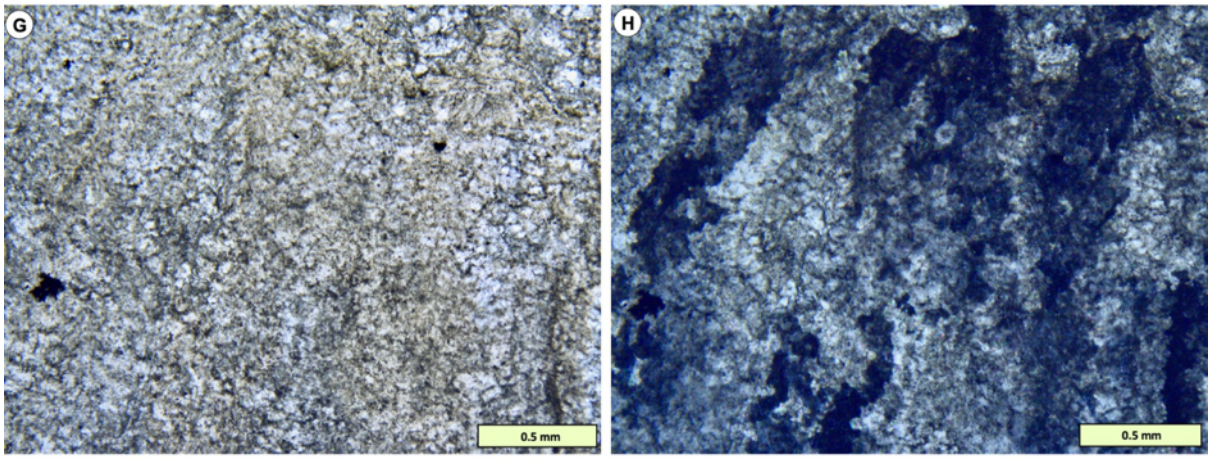

Fig. 8-4G-H. Further enlargement of VS showing the skeletal structure of *Pachystroma hesslandi* is made or a fine network, that has elongate overprinting diagenetic crystals in XPL. File: 24-04-K-13-Cut

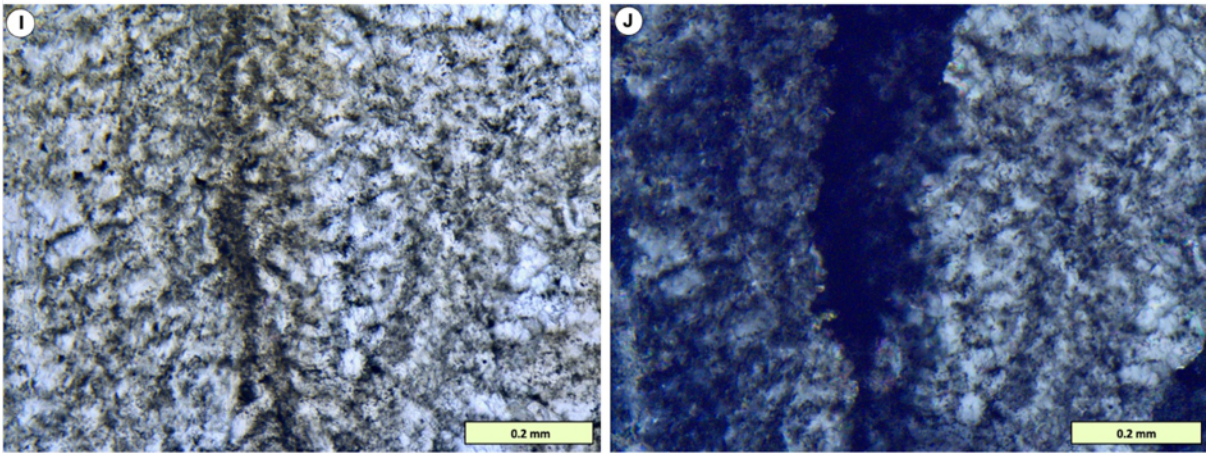

Fig. 8-4I-J. Higher resolution view of VS in PPL and XPL. File: 24-05-K-13-Cut

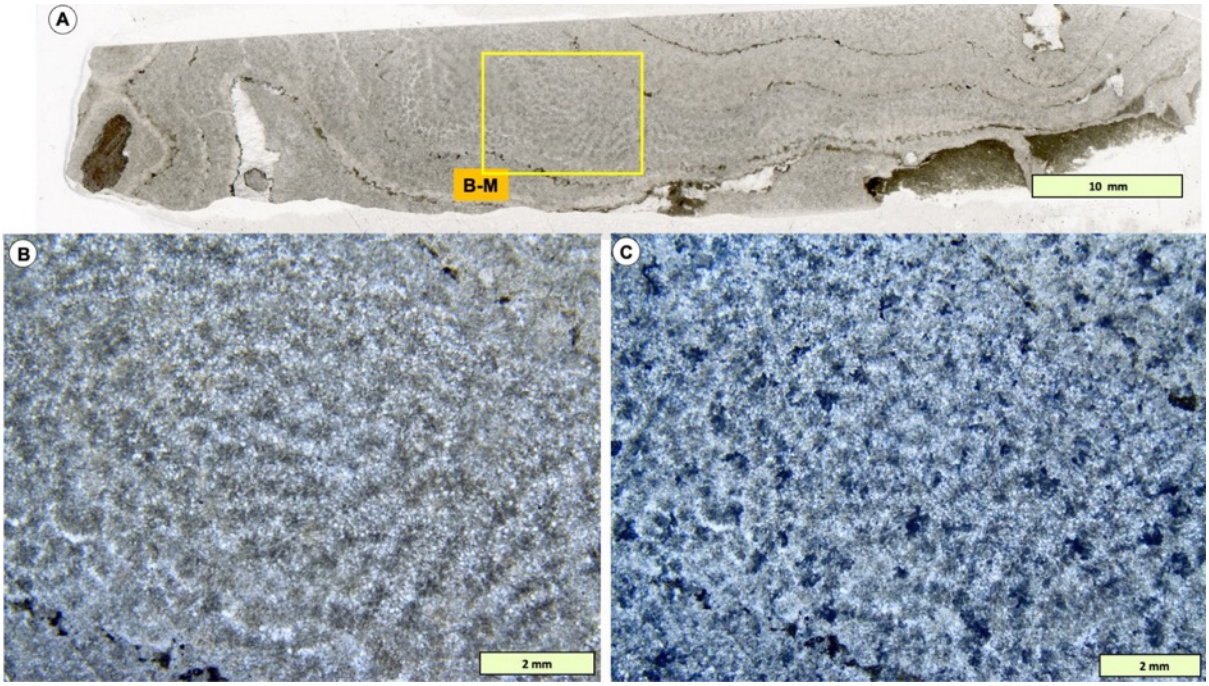

Fig. 8-5A-C. TS of *Pachystroma hesslandi* showing the vertical elements are clustered into vague pillar structures; overprinting in XPL shows the elongate crystals of the previous VS views are irregular elongate crystals that are more-or-less equant in TS, thus are consistent with the description of them as being approximately club-shaped; this is the same as in nearly all other stromatoporoids. File: 24-06-K-13

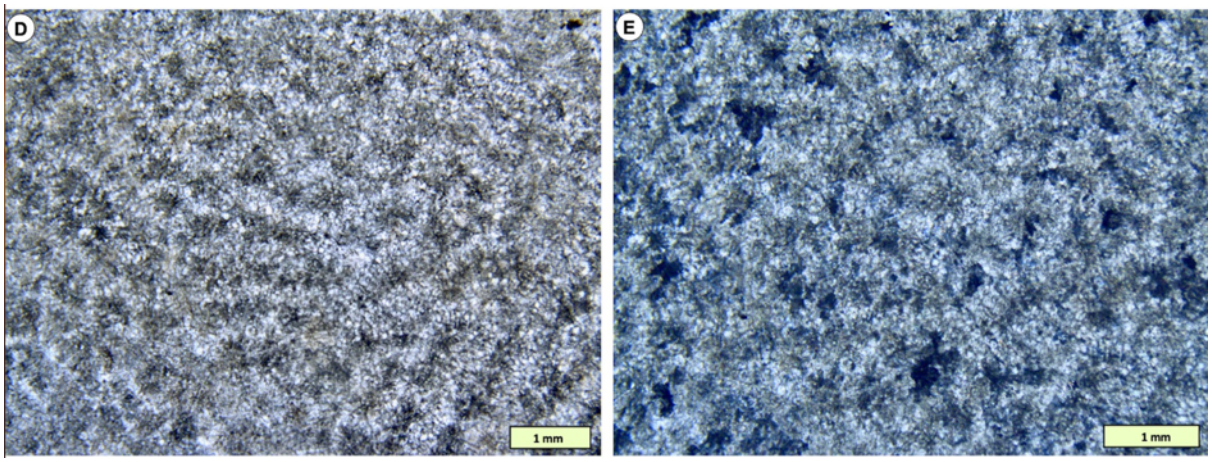

Fig. 8-5D-E. TS enlargement showing more details of *P. hesslandi* in TS. File: 24-07-K-13-Cut

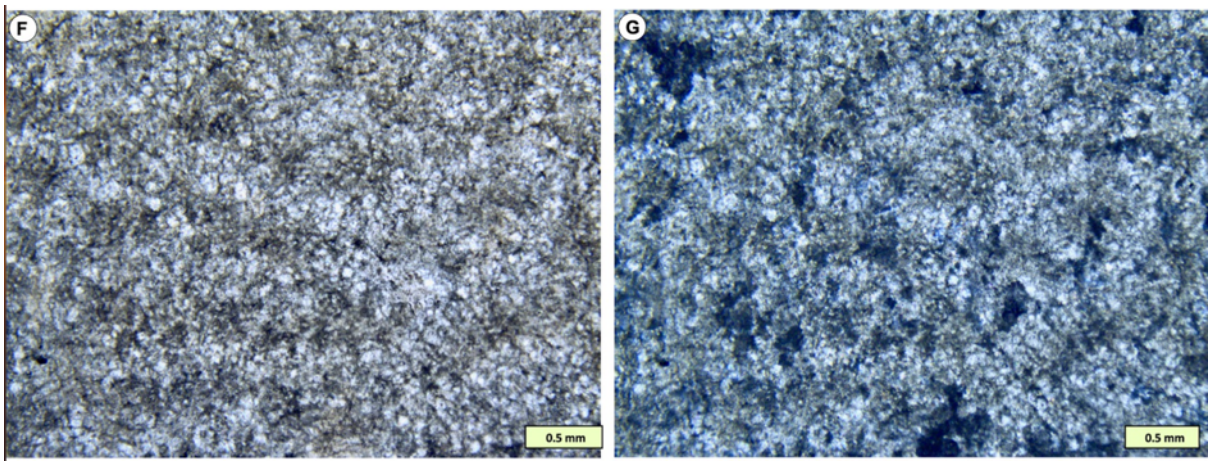

Fig. 8-5F-G. Further enlargements of previous figure. File: 24-08-K-13-Cut

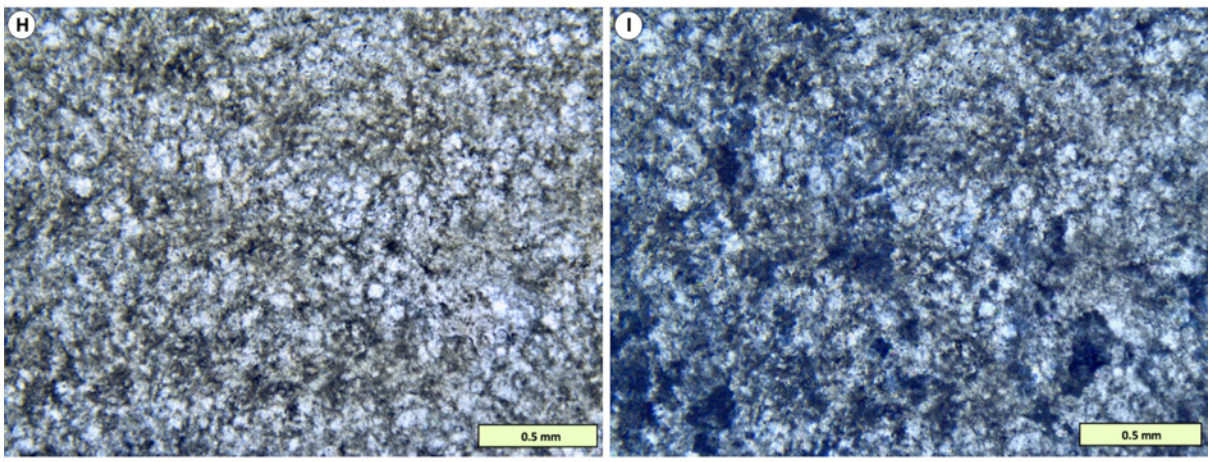

Fig. 8-5H-I. Higher-resolution TS views of previous figure, showing the network structure of *P. hesslandi* and the overprinting diagenesis in XPL. File: 24-09-K-13-Cut

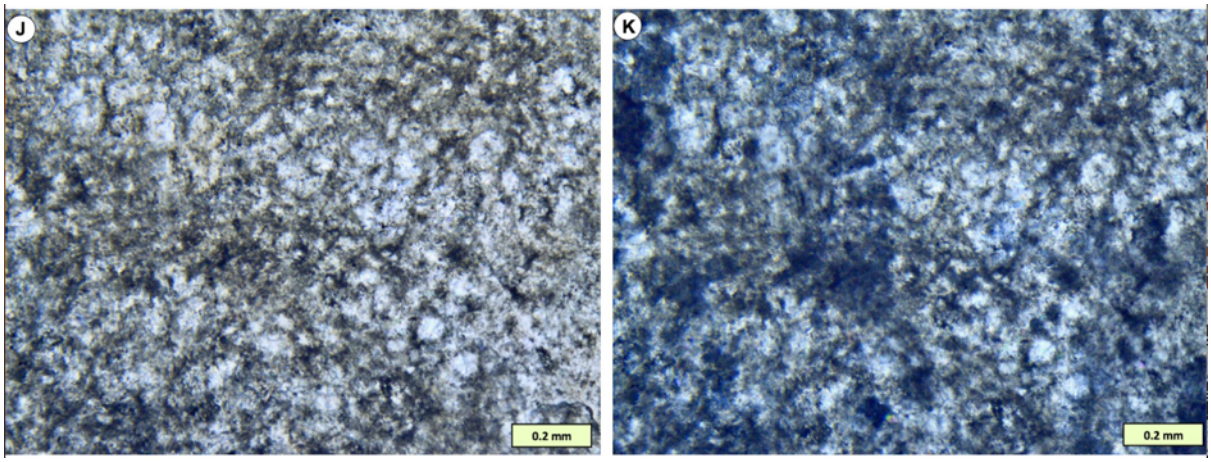

Fig. 8-5J-K. Fine details of *P. hesslandi* in TS. File: 24-10-K-13-Cut

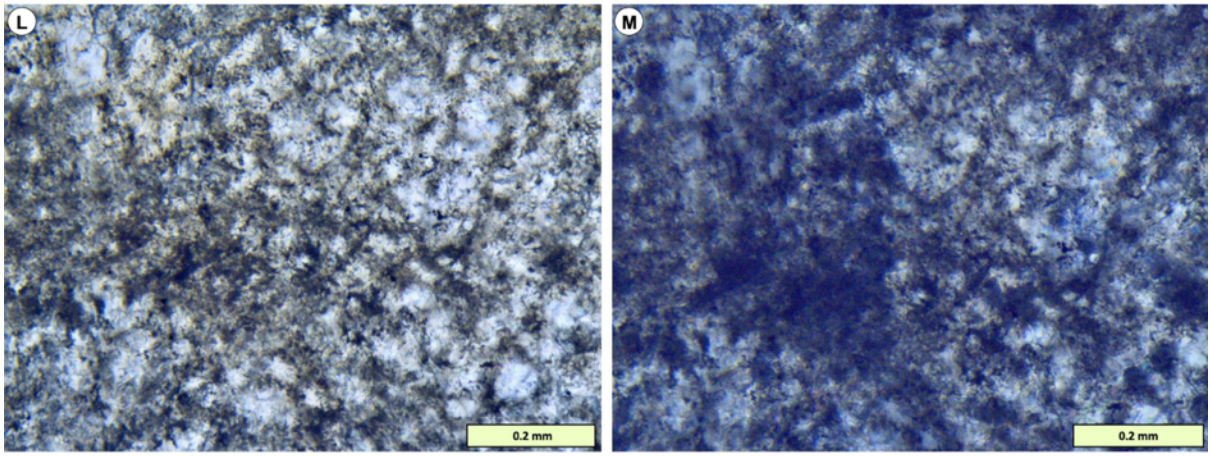

Fig. 8-5L-M. Highest resolution of *P. hesslandi* structure. File: 24-11-K-13-Cut

8.3. Pachystroma hesslandi (2nd sample), Upper Visby Fm, lowermost Wenlock, Silurian, Gotland

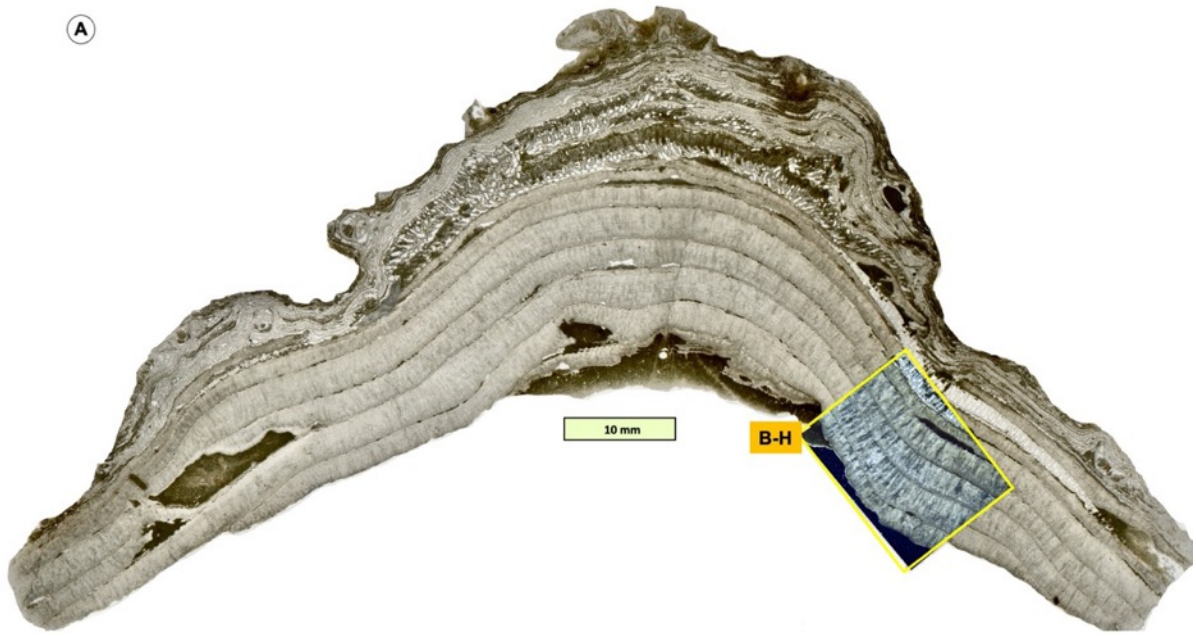

Fig. 8-6A. VS of whole thin section of another sample of *Pachystroma hesslandi* (*Ph)* showing a deep concavity on its base, indicating that it grew on a topographic high on the substrate. But look at the centre of the base, where the relationship between the stromatoporoid skeleton and the underlying substrate is very irregular in detail; this type of feature was interpreted by Kershaw et al. (2021, Facies paper) to indicate that the sediment was at least partially lithified and eroded before the stromatoporoid started to grow, and the shape of the concavity is an indication of sea-floor topography, of which the stromatoporoid took advantage. This image is one of many in the Palaeozoic history of stromatoporoids that give a clue that the sea floor was commonly at least partly lithified, before growth of benthic fossils such as stromatoporoids; this also can be seen in tabulate and compound rugose corals. In this photo, the *Ph* shows numerous growth interruption surfaces, commonly called latilaminae in stromatoporoid terminology. Note that latilaminae are simply growth pauses in the development of a stromatoporoid that are most likely due to growth interruption, and commonly there is sediment along the interruption, as can be seen by the thin dark lines and patches in this photo. There are at least 6 growth interruption events in the *Ph*. Lower right is a superimposed XPL image to show the locations of B-H below. The *Ph* is then encrusted by a colonial skeletal organism, looks like a bryozoan, and another stromatoporoid (*Petridiostroma simplex*) at the top. Upper Visby Formation, lower Wenlock, Silurian; Häftingsklint, northern Gotland, Sweden. 25-1-HA34-i-Ph-VS

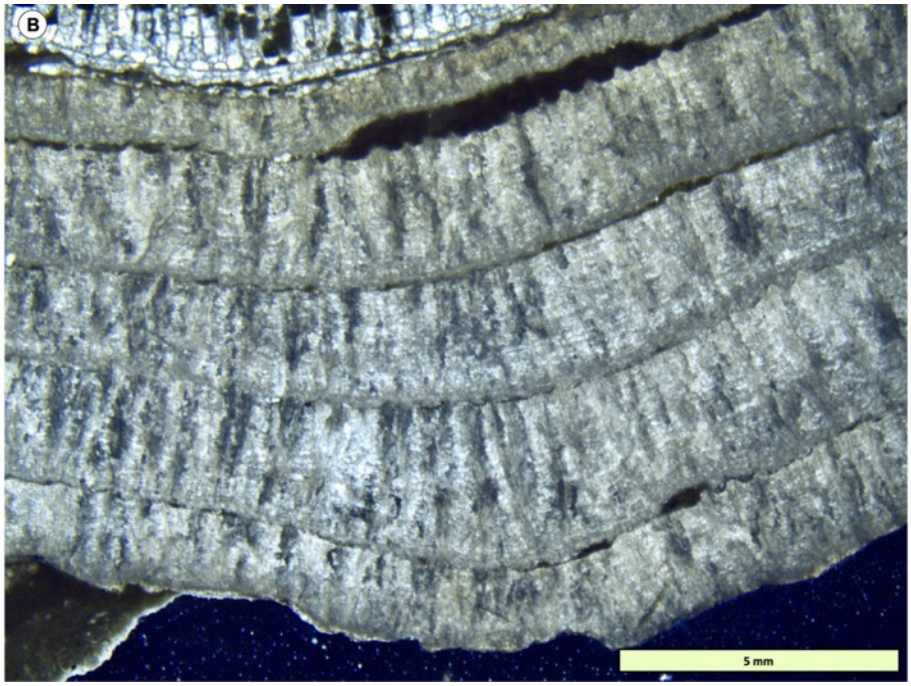

Fig. 8-6B. Enlargment of box in A, showing the irregular basal surface of the *Ph*, as described in the caption in A; there are 4 growth interruption events and then the final layer of the *Ph* died (likely due to sedimentation as a final growth interruption!) and was encrusted by a bryozoan. The growth interruptions are identified by tiny amounts of sediment scattered along the interruption lines; the 4th interruption was larger, and there are tiny papillae visible on the *Ph* surface of the sediment pocket upper centre. Papillae are also visible at the top of the second growth where there is the second interruption surface, slightly below centre of this picture. These papillae seem to relate to the large elongate crystals in extinction that run through each layer, and thus have some comparability to the diagenetic structure of *Ls*. File: 25-2-HA34-i-Ph-VS

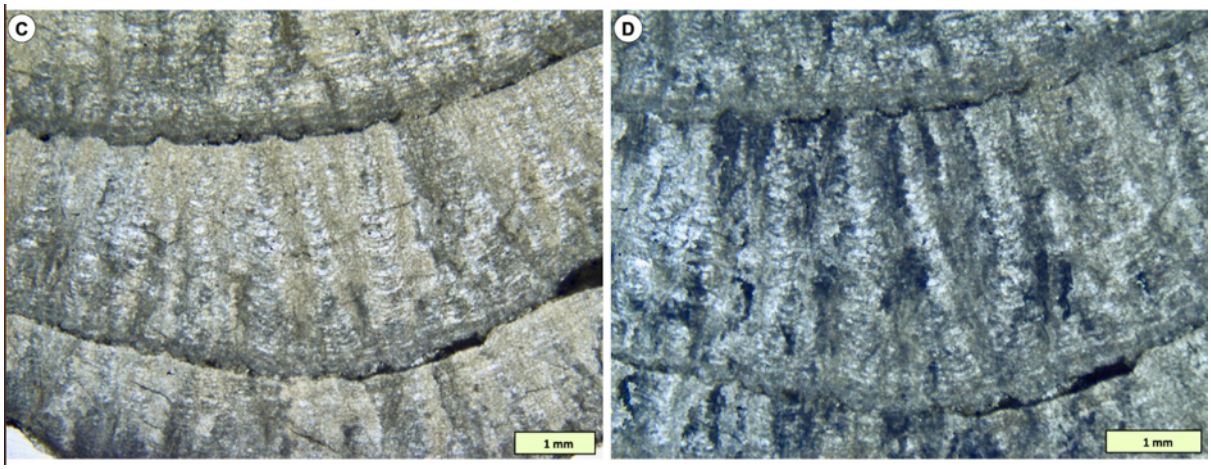

Fig. 8-6C-D. Enlargement of the centre of previous photo showing more detail of the elongate extinct calcite diagenetic crystals, that coincide with papillae picked out on the upper interruption event. File: 25-3-HA34-i-Ph-VS-Cut

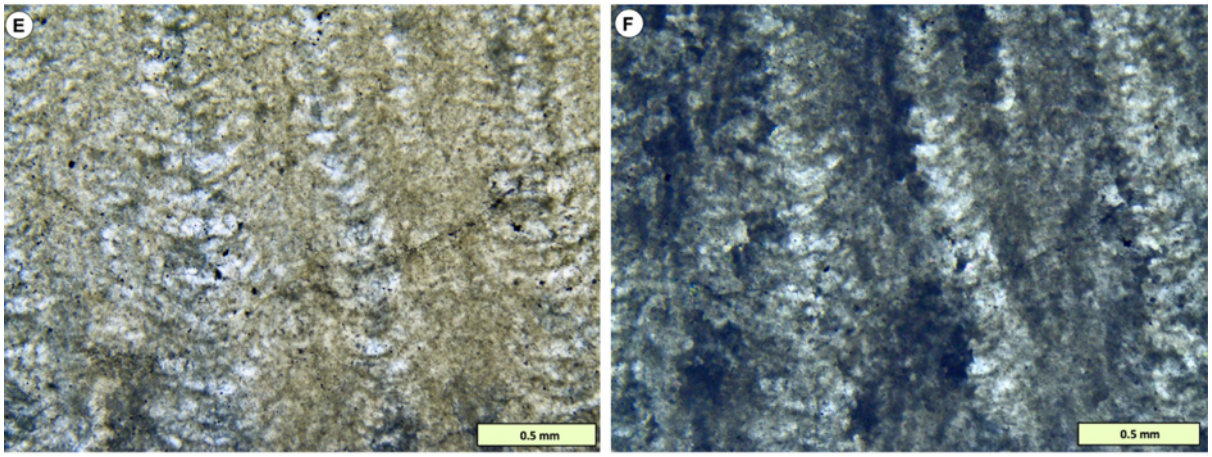

Fig. 8-6E-F. Enlargement of PPL and XPL structure of *Ph*, showing the network construction of the skeleton of *Ph*, with concentration into pillar-like structures that are the focus of the extinct crystals. File: 25-4-HA34-i-Ph-VS-Cut

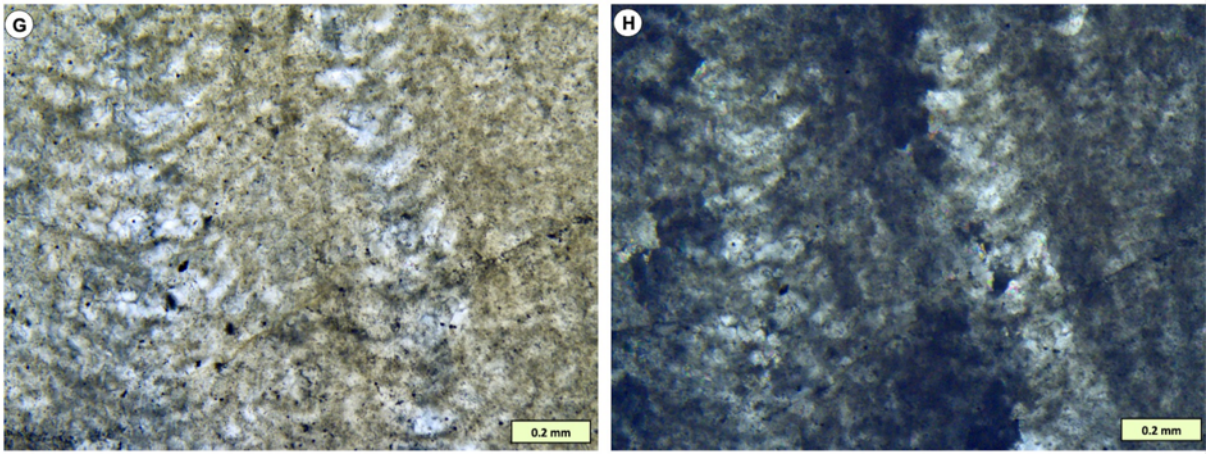

Fig. 8-6G-H. Further enlargements in PPL and XPL of the network structure and diagenetic character of *Ph*. File: 25-5-HA34-i-Ph-VS-Cut

8.4. "Labechia rotunda", Much Wenlock Limestone formation, Wenlock, Silurian, England

Labechia rotunda is a taxon named in a paper by by Mary Johnston in 1915, but unfortunately was done so directly from the hand specimen and no thin sections were made (can you believe it ??!!). In 1960's Kei Mori visited the Natural History Museum, where Johnston's material is stored and got permission to make thin sections; Mori (1970) reported that its structure looks more like *Lophiostroma schmidii* and thus named it as such. In 2019 I found the thin sections and photographed them for the first time, the images were presented in Kershaw et al. (2021, British Silurian stromatoporoids monograph, published by the Palaeontographical Society). The images were made available in a different format in the Natural History Museum Data Portal, at:
Https://data.nhm.ac.uk/dataset/british-silurian-stromatoporoid-systematic-palaeontology

Those NHM images are displayed in Fig. 8.7. The PPL views show very little, but the XPL views demonstrate without doubt this is *Lophiostroma schmidtii*. Fig. 8.7E particularly shows the upward-curving character of the diagenesis, comprising crystal fans and aggrading neomorphic overprint, that is absolutely characteristic of the images of *Ls* illustrated in this atlas. So there is no question about its taxonomy; thus *Labechia rotunda* is invalid, and Johnston's sample is *Ls.*

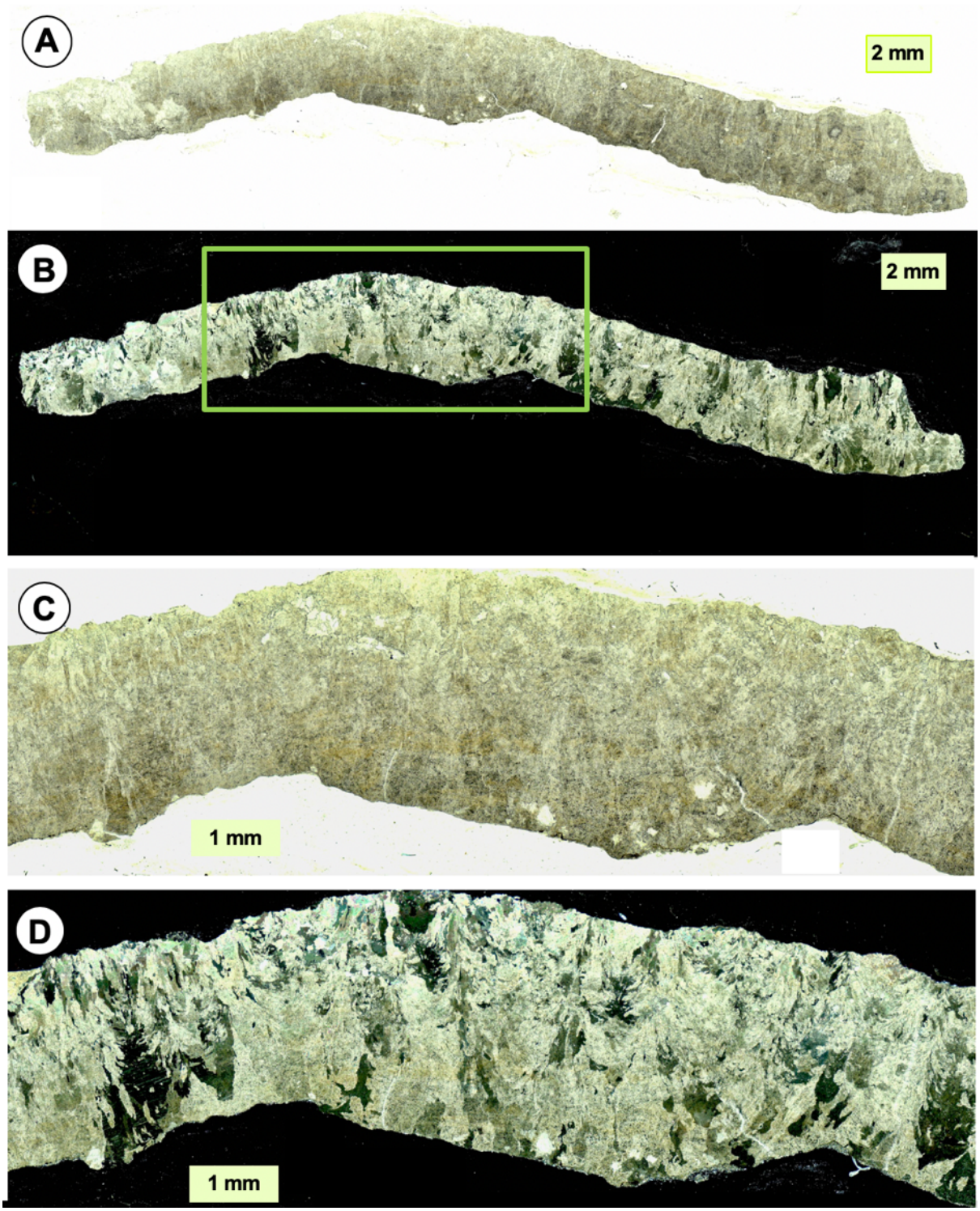

Fig. 8-7A-D. VS views. The PPL views show poor preservation but in XPL the character of *Ls* is clearly revealed. File: 25-6-2a-LabechiaRotunda-VS-NHM-DataPortal

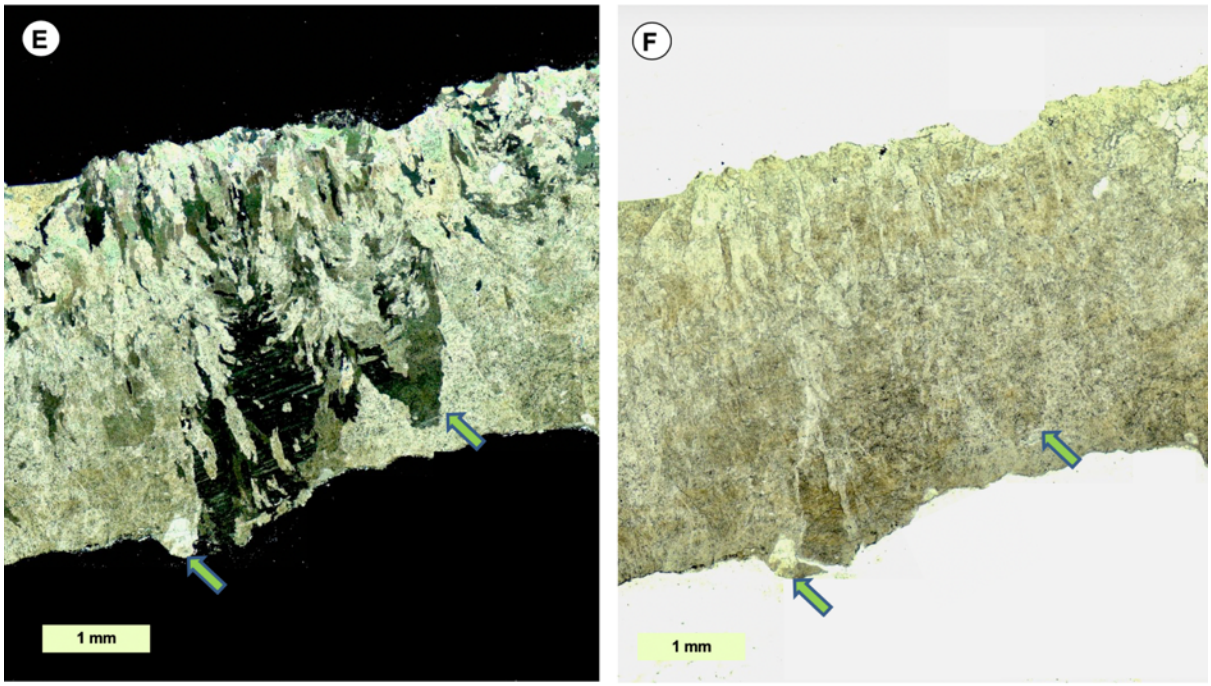

Fig. 8-7E-F. Enlarged VS views. XPL view shows the diagenetic features of crystal fans and overprinting aggrading neomorphic structure. File: 25-7-2b-LabechiaRotunda-VS-NHM-DataPortal

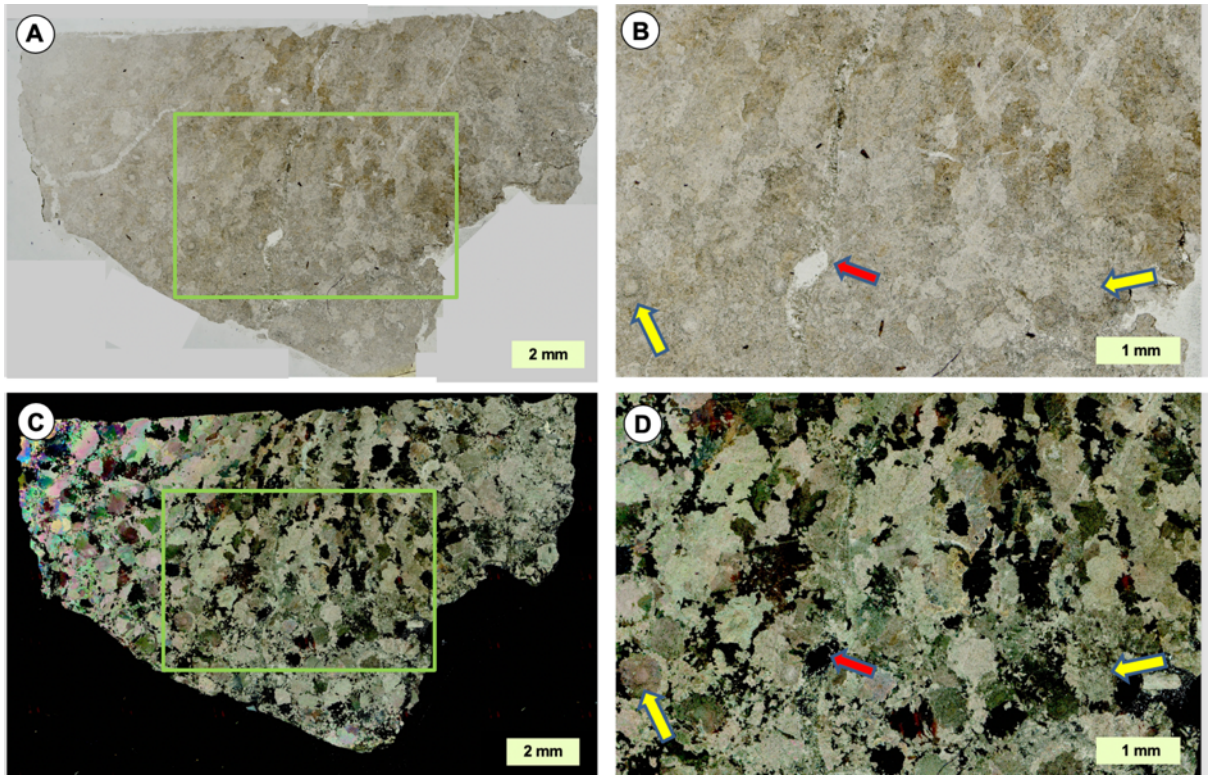

Fig. 8-8A-D. TS views show the PPL sections are too poorly preserved to show anything useful, but the XPL views, in combination with the VS views in the previous figures make it very clear that this is *Ls.* File: 25-8-2c-LabechiaRotunda-TS-NHM-DataPortal

8.4. "Labechia scabiosa", Much Wenlock Limestone formation, Wenlock, Silurian, England

Like *Labechia rotunda*, *Labechia scabiosa* was named by Nicholson in his monograph of British Stromatoporoids published in 4 parts between 1886-1892. But this taxon was named directly from the hand specimen, without making thin sections. However, Mori's visit to the NHM in 1960's led to thin sections being made, as for *L. rotunda* discussed in the previous case. Mori (1970) also considered *L. scabiosa* as being *Lophiostroma schmidtii*, but as for *L. rotunda* did not figure it. So below are images of *L. scabiosa*, that are also published in Kershaw et al. (2021 British Silurian stromatoporoids monograph). Those images were also presented in a different format in the Natural History Museum Data Portal at:
Https://data.nhm.ac.uk/dataset/british-silurian-stromatoporoid-systematic-palaeontology
These are reproduced here.
This stromatoporoid is very poorly preserved. In PPL the structure is effectively impossible to analyse and it is not much better in XPL. The VS XPL does not show the upward-curving character of the crystal fans, but it does show the overprinting of FRIC as large crystals normal to the growth layers, so there is no doubt this is a stromatoporoid. Nevertheless, in TS the XPL view shows the circular cross sections that are characteristic of *Ls*, so the most likely taxon is *Ls*. However, we must be careful here because it is very poorly preserved, and was a bad choice as a new taxon!!!!

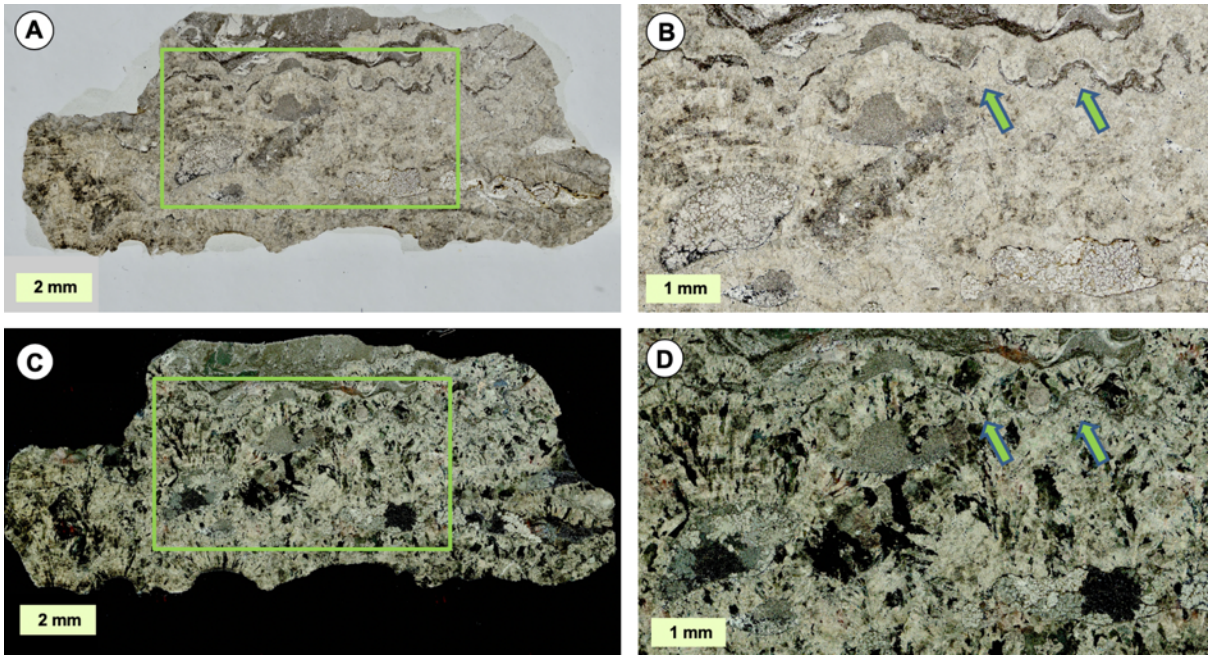

Fig. 8-9A-D. VS views in PPL and XPL. The XPL views do not show this is *Lophiostroma schmidtii.*
File: 25-9-3b-LabechiaScabiosa-VS-NHM-DataPortal

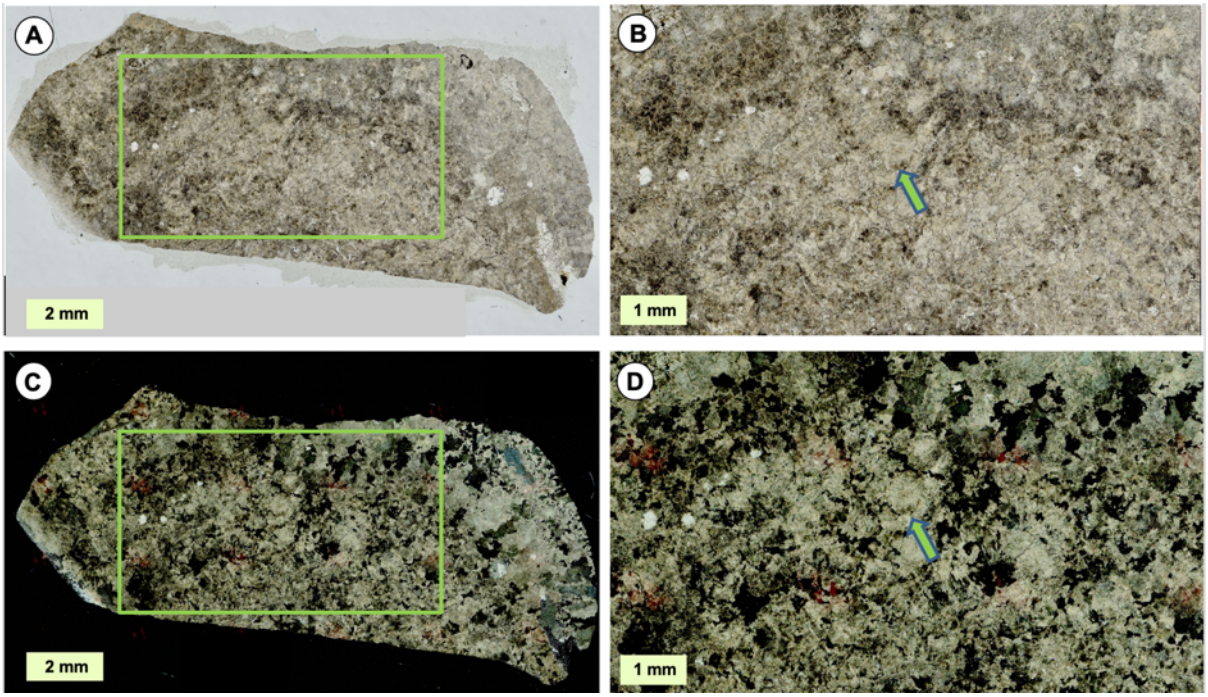

Fig. 8-10A-D. TS views, note D shows poorly preserved TS structure of *Lophiostroma schmidtii* (green arrow), so the most reasonable identification is *Ls*, although this is a very poorly preserved stromatoporoid. 25-103a-LabechiaScabiosa-TS-NHM-DataPortal

SECTION 9:
Gypsum in Kuppen biostromes

Earlier in this atlas I talked about the problem of determining the palaeoenvironment of the biostromes that contain the samples of *Ls* illustrated here. I mentioned the presence of gypsum and gypsum pseudomorphs in the biostrome, and this last section of data presentation are two samples that show the presence of gypsum evaporites. These images are presented as very scant evidence that might shed light on the nature of the ancient environment of the biostromes. Note the biostromes occur across a large area of eastern Gotland and formed on a flat seabed in a quiet environment, in shallow conditions. The possibility exists that the biostromes developed in a setting of raised salinity, and if so this might explain the unusual high concentration of stromatoporoids in these deposits. Of course the resistance of stromatoporoids to raised salinity is unknown, but this section is included to make the point that it is possible. Two examples are provided. This idea is very preliminary and would require a consistent search for more evidence that may or may corroborate this idea.

9.1. Gypsum in sediment associated with Plectostroma scaniense

This example was published in 1987 in GFF, and here are the pictures in colour, in contrast to the monochrome pictures in the journal.

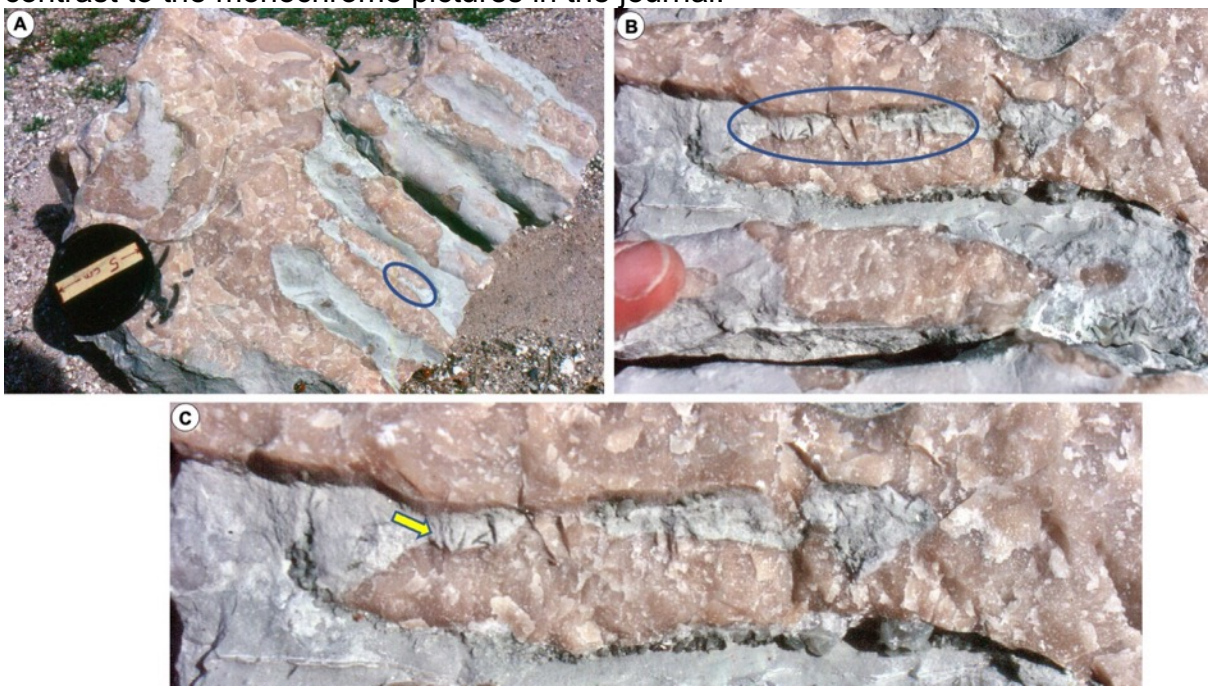

Fig. 9-1A-C. Field views of *Plectostroma scaniense* with small lath-shaped crystals in the sediment next to the stromatoporoid. File: 22-1-Gypsum-Kuppen

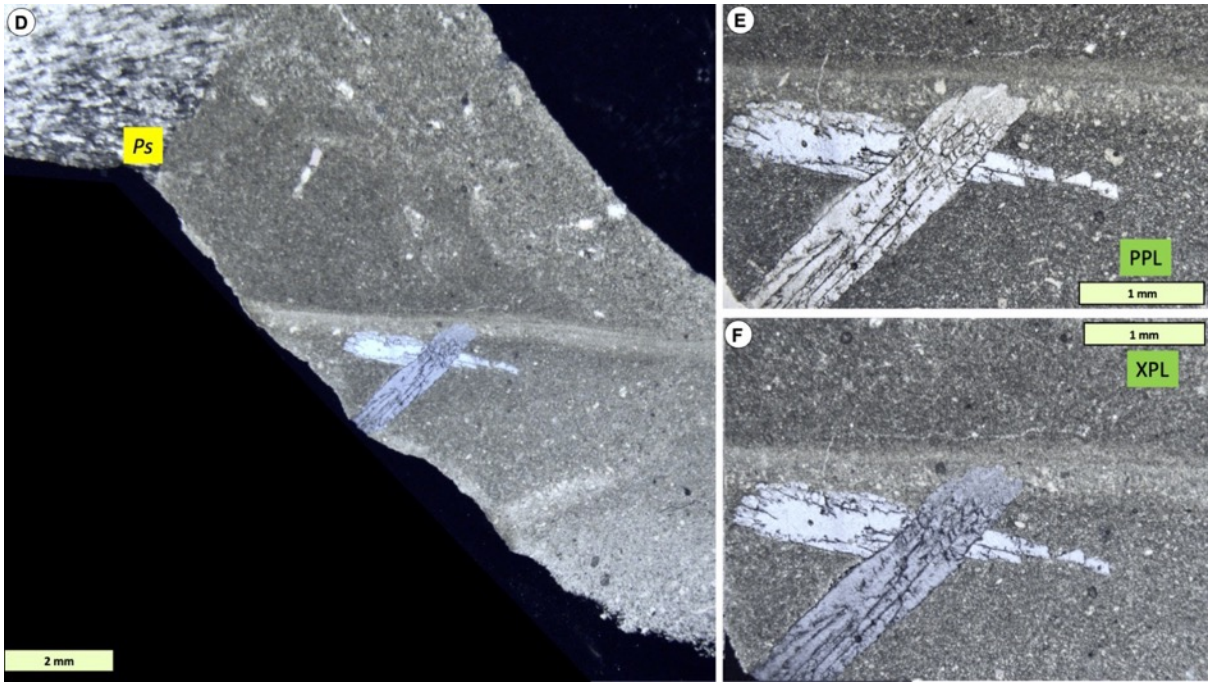

Fig. 9-1D-E. Thin section views of the gypsum crystals and sedimentary layering next to Ps. File: 22-2-Gypsum-Kuppen

9.2. Gypsum in sediment associated with Lophiostroma schmidtii

This example turned up during the study for this atlas and shows sediment next to *Ls* where gypsum and gypsum pseudomorphs are preserved.

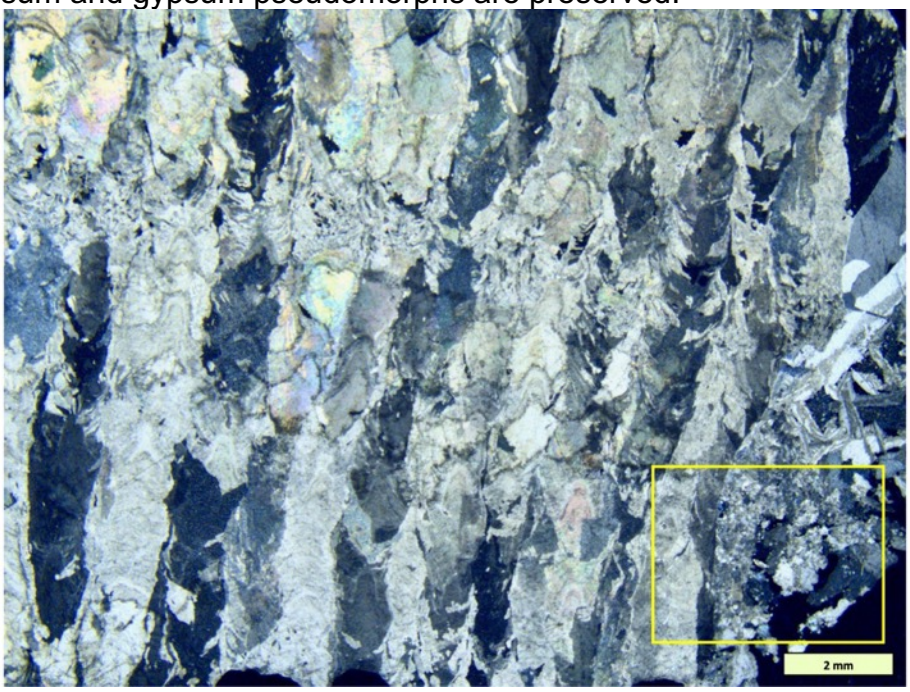

Fig. 9-2. VS XPL view of *Ls* that is a repeat of part of Case Study 10 in Section 6.10. This image shows the diagenetic structure of vertically-orientated large crystals. Lower right corner (yellow box) shows area of Fig. 9.3A, that illustrates gypsum in cavity cement on the edge of the sample. File: 22-2b-Gypsum-Kuppen

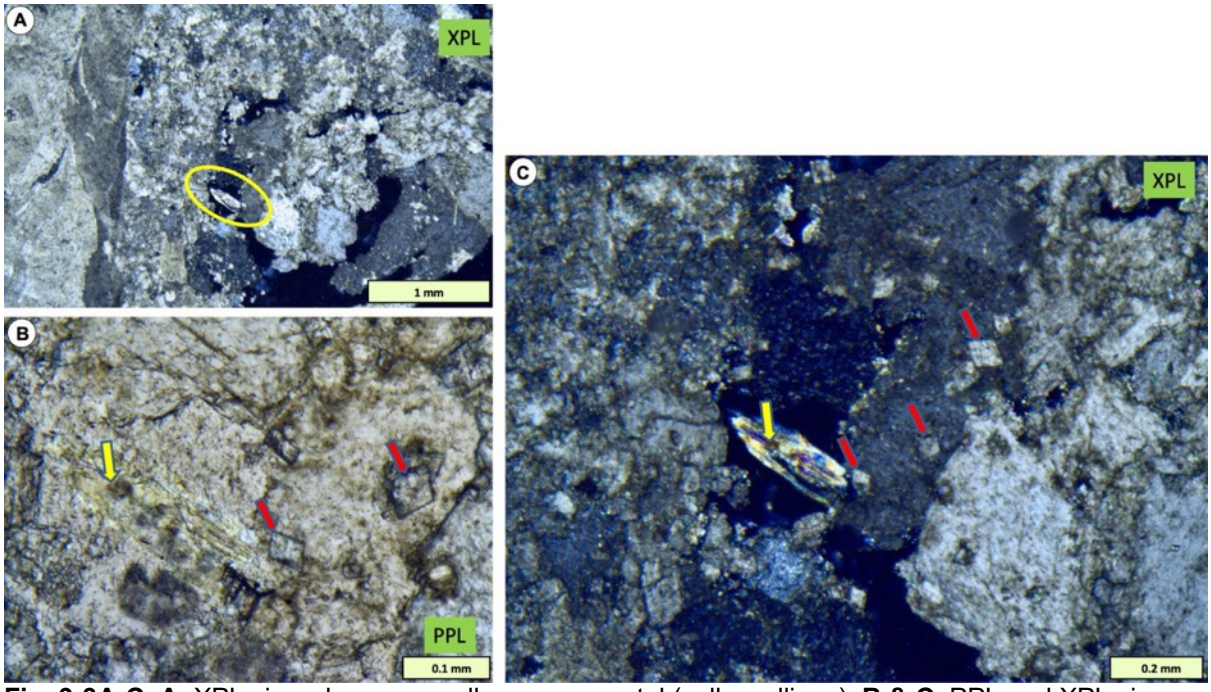

Fig. 9-3A-C. A. XPL view shows a small gypsum crystal (yellow ellipse). **B & C.** PPL and XPL views with matched points arrows showing detail of gypsum crystal (yellow arrow) and dolomite rhombs (red arrows), that would be expected to be present in a condition of raised salinity. File: 22-3-Gypsum-Kuppen

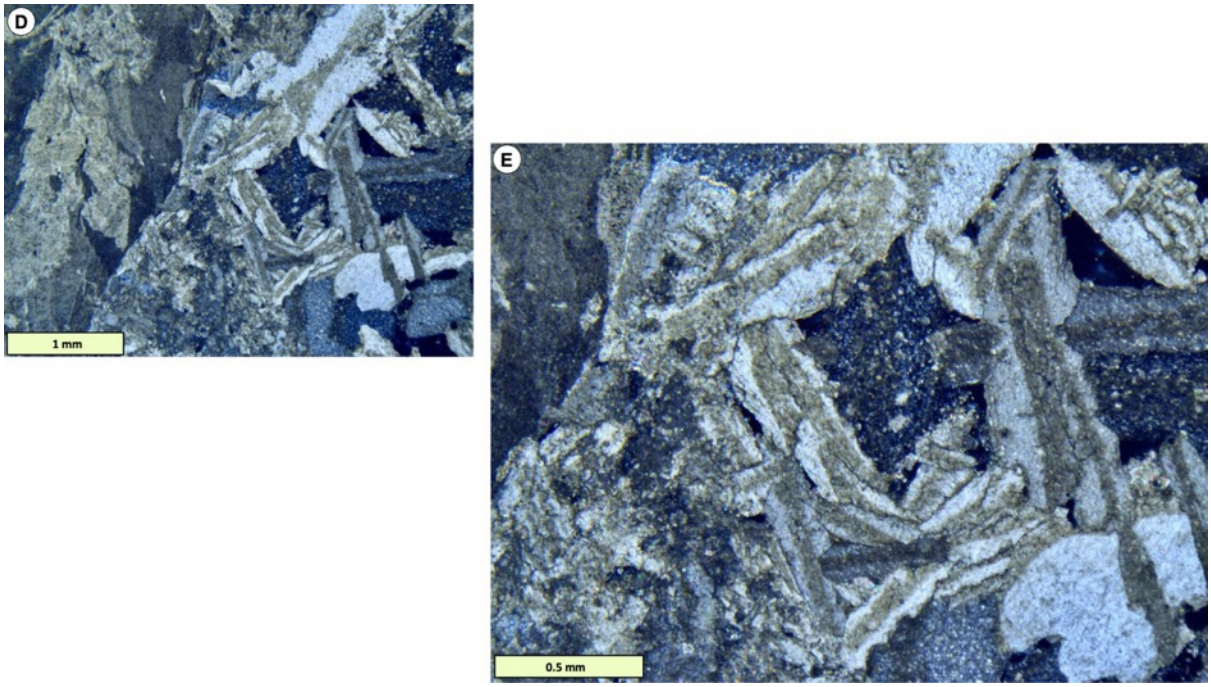

Fig. 9-2D-E. Enlargement of the area above the yellow box in A, showing gypsum pseudomorphs in calcite. File: 22-4-Gypsum-Kuppen

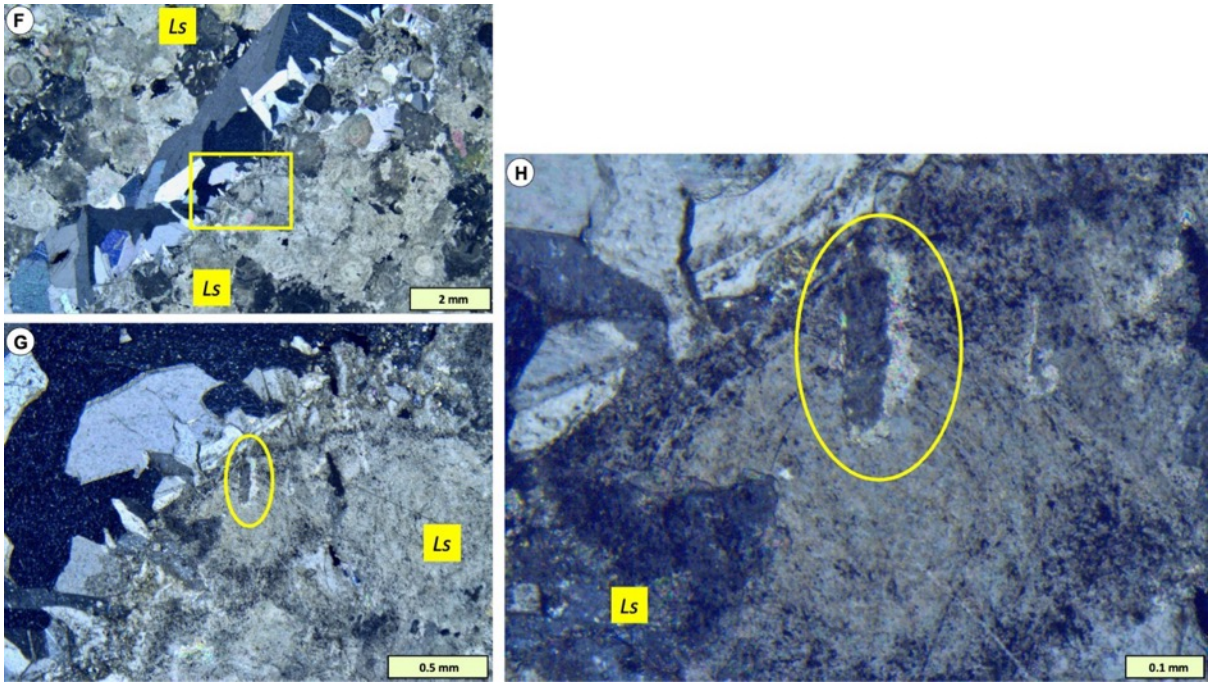

Fig. 9-2F-H. Enlargement of the TS thin section of this sample that shows what looks like a gypsum pseudomorph within the the *Ls* structure, and may be evidence of a diagenetic alteration of the *Ls* that is not seen in other samples. File: 22-5-Gypsum-Kuppen

SECTION 10:
CONCLUSION

This detailed study of *Lophiostroma schmidtii* (*Ls*) revealed to me more depth of understanding of stromatoporoids, their structure, diagenesis and taxonomy. Key points that emerge from this study are:

1) It remains the best option to keep *Ls* within the stromatoporoids given its similarity of growth form and growth features of primary cavities, substrate, growth interruption to all other stromatoporoids;
2) *Ls* has a diagenetic character that follows the general pattern of stromatoporoids – that is, FRIC, but also that its diagenesis is more complicated than other stromatoporoids. Other stromatoporoids basically have a single form of overprinting of FRIC onto the skeleton, but *Ls* has **three** (vaguely-fibrous calcite, 3D crystal fans and aggrading neomorphism): this is amazing, and sets *Ls* apart from other stromatoporoids.
3) XPL is really important in understanding processes in stromatoporoids; so the traditional approach of studying stromatoporoids in plain/plane light is only ever going to give part of the story. XPL needs to be used in a routine way, and therefore thin sections need to be thinner. So stromatoporoid study should be made using not just the standard over-thick sections to show their taxonomic details, but thinned sections, maybe as thin as 20 microns or less in some cases, to extract all the petrographic characters.
4) Because of the similarities and differences between *Ls* and other stromatoporoids, *Ls* effectively gives a way to place stromatoporoids in a diagenetic perspective;
5) In this study, CL has proved particularly useful, because the evidence from co-occurring fossils (brachiopods, crinoids that are well-preserved) is that CL is likely to reveal something like the original stromatoporoid structure, certainly more clear to see than PPL. In the case of *Ls*, CL proves very useful to understand its structure, and relationship to diagenesis;
6) Thus it could be that the future of stromatoporoid taxonomy is to use CL as a routine tool. My work on stromatoporoids using CL in diagenetic studies (Kershaw et al. 2021, Facies paper) shows the value of using CL in diagenesis, but this atlas extends that to demonstrate its potential value in taxonomy

I hope you have enjoyed reading this as much as I have done writing it.

Steve Kershaw